

78p.

71

N64-17685

CODE-1

TMX-51312

MTP-RP-64-1)
January 14, 1964

NASA

GEORGE C. MARSHALL

**SPACE
FLIGHT
CENTER,**

HUNTSVILLE, ALABAMA

DISTRIBUTION OF UNBOUND CHARGED PARTICLES
IN THE STATIC MAGNETIC FIELD OF A DIPOLE

By Arthur D. Prescott

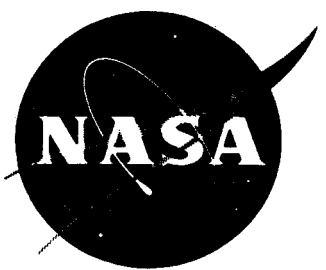
14 Jan. 1964 788 n/s

(NASA TMX-51312;)

OTS: PRICE

\$ 7.60 ph
\$ 2.54 mf

XEROX
MICROFILM



DISTRIBUTION OF UNBOUND CHARGED PARTICLES
IN THE STATIC MAGNETIC FIELD OF A DIPOLE

By Arthur D. Prescott

ABSTRACT

17685 A

The distribution of relativistic unbound charged particles in the static magnetic field of a dipole with respect to a monoenergetic, isotropic, time independent homogeneous distribution at infinity is determined by assuming Liouville's theorem and the Störmer theory of allowed and forbidden regions for unbound particle motion. For an isotropic distribution, the allowed solid angle for particle motion at any given point (r, θ, ϕ) in the field is determined by mapping point (r, θ, ϕ) into the allowed and forbidden regions of Störmer space, via the Störmer transformation, at a particular particle impact parameter. The totally and partially shielded regions are defined and are examined with particular emphasis on the shielding effectiveness of the partially shielded region to charged particles. The volumes of the totally and partially shielded regions are numerically computed. Once the totally and partially shielded regions are established, the momentum cutout in momentum space at point (r, θ, ϕ) is determined by mapping the point into the totally, partially, and unshielded regions in Störmer space with particle momentum as a variable. These methods are then used to compute the proton flux ratio at points on the surface of a spherical spaceship as a function of particle kinetic energy.

The theory is applied to the dipole field of a finite current loop and a study of the totally and partially shielded regions shows that the partially shielded region provides protection in the high energy regime where the totally shielded region is effectively nonexistent.

Arthur

GEORGE C. MARSHALL SPACE FLIGHT CENTER

MTP-RP-64-1

DISTRIBUTION OF UNBOUND CHARGED PARTICLES
IN THE STATIC MAGNETIC FIELD OF A DIPOLE

By Arthur D. Prescott

NUCLEAR AND PLASMA PHYSICS BRANCH
RESEARCH PROJECTS LABORATORY

ACKNOWLEDGMENTS

The author wishes to acknowledge his indebtedness to his associates for their encouragement and interest during the preparation of this report. The discussions and criticisms of Mr. E. W. Urban and Dr. R. D. Shelton were particularly helpful.

Mr. Johnny Watts and Mr. Tracey Price helped with the programming of equations for the IBM 7090 and the RecompII computers.

TABLE OF CONTENTS

	Page
I. INTRODUCTION	2
II. STÖRMER THEORY SUMMARY	3
A. General Equations of Charged Particle Motion in a Static Magnetic and a Static Electric Field	3
B. Charged Particle Motion in a Steady State Dipole Magnetic Field	4
C. Störmer Space and Related Topics	9
III. PARTICLE DISTRIBUTION IN THE MAGNETIC FIELD OF AN INFINITESIMAL DIPOLE	14
A. Liouville's Theorem and its Application to a Static Magnetic Field	14
B. Monoenergetic, Isotropic, Homogeneous Distri- bution at an Infinite Distance Away From the Dipole	17
C. Dependence of the Forbidden Regions on Impact Parameters	19
D. Isotropic, Continuous Energy Distribution Homo- geneously Distributed an Infinite Distance Away From the Infinitesimal Dipole	27
1. Integrated Differential Number Spectrum or Flux Spectrum	27
2. Differential Number Spectrum	34
3. Volume Integral of the Particle Density and Shielding Effectiveness of the Partially Shielded Region	37
4. Constant Flux Surfaces	40
IV. PARTICLE DISTRIBUTION IN THE MAGNETIC FIELD OF A FINITE CURRENT LOOP	46
A. Isotropic, Continuous Energy Distribution Homo- geneously Distributed an Infinite Distance Away From the Current Loop	46
APPENDIX	60

LIST OF ILLUSTRATIONS

<u>Figure</u>	<u>Title</u>	<u>Page</u>
1	Reference Coordinate System	6
2	Allowed and Forbidden Regions for Three Select Values of $\bar{\gamma}$ in the (ρ, θ) Plane	10
3	Particle Störmer Radius for Protons, Electrons, and Alpha Particles in the Earth's Magnetic Field, $M = 1.01788 \times 10^{17}$ weber-meters, vs Kinetic Energy	12
4	Particle Störmer Radius for Protons and Electrons vs Kinetic Energy, with Magnetic Dipole Moment as a Parameter	13
5	Allowed and Forbidden Regions in the (ρ, θ) Plane for $\bar{\gamma} = -1.0$	21
6	Shielded Regions of an Infinitesimal Magnetic Dipole Field in the (ρ, θ) Plane	24
7	Mapping of Point (r, θ) into the (ρ, θ) Plane via the Störmer Transformation	29
8	Arbitrary Flux Spectrum at \vec{r} and \vec{r}_∞	30
9	Cone Half Angle Above the Eastern Horizon of a 20-meter Sphere for Protons vs Cutoff Energy. The Infinitesimal Dipole is Located at the Center of the Sphere.	32
10	Cone Half Angle above the Eastern Horizon of a 20-meter Sphere for Protons vs Cutoff Energy. The Infinitesimal Dipole is Located at the Center of the Sphere.	33

LIST OF ILLUSTRATIONS (contd.)

<u>Figure</u>	<u>Title</u>	<u>Page</u>
11	Relativistic Proton Flux Ratio Ten Meters From a Dipole at Select Magnetic Co-latitudes	35
12	Relativistic and Nonrelativistic Proton Flux Ratio Ten Meters from a Dipole on the Magnetic Equator	36
13	Constant Flux Ratio Curves in the Equatorial Plane of the Earth Vs Proton Kinetic Energy	43
14	Constant Flux Contours for Unbounded 1 Bev, 100 Mev and 1 Mev Protons in the Field of an Infinitesimal Magnetic Dipole	44
15	Allowed and Forbidden Regions of Particle Motion in the (ρ', θ) Plane for Three Select Values of $\bar{\gamma}$ with $\lambda = 0.02$	49
16	Relativistic Proton Flux Ratio Ten Meters from a Current Loop with a Radius of Ten Meters at $\bar{\theta} = 20^\circ$	54
17	Relativistic Proton Flux Ratio Ten Meters from a Current Loop with a Radius of Ten Meters at Select $\bar{\theta}$	55
18	Shielded Regions in the (ρ', θ) Plane of a Finite Current Loop	56
19	Limits of the Totally Shielded Region and Partially Shielded Region in the Plane of the Loop	57
20	Constant Flux Contours in the (r, θ) Plane for Unbound Charged Particles Around a 10-meter Current Loop with a Dipole Moment $M = 2.51 \times 10^5$ weber-meters	59

LIST OF SYMBOLS

L	Lagrangian
T	particle kinetic energy
U	generalized velocity dependent potential
q	quantity of charge carried by a particle
\vec{A}	magnetic vector potential
ϕ_E	electrostatic scalar potential
\vec{v}	particle velocity vector
r	radial coordinate in spherical coordinates
θ	polar angle in spherical coordinates
ϕ	azimuthal angle in spherical coordinates
A_r	r -component of the magnetic vector potential
A_θ	θ - component of the magnetic vector potential
A_ϕ	ϕ - component of the magnetic vector potential
m	particle mass
P_ϕ	canonical momentum conjugate to the ϕ coordinate
H	Hamiltonian
\vec{F}	Lorentz force vector
\vec{E}	electric field vector
v_ϕ	ϕ - component of the particle velocity

p	magnitude of the linear mechanical momentum vector
v	particle speed
\vec{M}	magnetic dipole moment vector
M	magnitude of the dipole moment vector
\vec{r}	radius vector in spherical coordinates
ρ	radial coordinate in spherical coordinates in Störmer space
c	speed of light in a vacuum
r_E	radius of the earth in real space
ρ_E	radius of the earth in Störmer space
q_i	generalized coordinate
P_i	generalized momentum conjugate to q_i
$f(\vec{r}, \vec{P})$	distribution function of particles in 6-dimensional phase space
t	time
\vec{p}	mechanical momentum vector
$\hat{\Omega}$	unit solid angle vector
$\Phi(\vec{r})$	flux density at point \vec{r}
$\vec{\rho}$	radius vector in Störmer space
R	radial coordinate in cylindrical coordinates
z	z-coordinate in cylindrical coordinates
ϕ	azimuthal angle in cylindrical coordinates

k	elliptic integral argument
a	current loop radius
I	current
$\delta [T-T_0]$	Dirac delta function
$K(k)$	complete elliptic integral of the first kind
$E(k)$	complete elliptic integral of the second kind
$B(k)$	special complete elliptic integral
$C(k)$	special complete elliptic integral
$D(k)$	special complete elliptic integral
ρ'	radial coordinate in Störmer space normalized by λ
$\tilde{\rho}$	radial coordinate Störmer space measured from the current loop
$\tilde{\theta}$	polar angle measured from the perpendicular to the plane of the current loop at the current loop
\tilde{r}	radial coordinate in real space measured from the current loop
μ_0	permeability of free space
δ_{ij}	Kronecker delta function
h_i	coordinate scale factor corresponding to the i^{th} coordinate
m_0	particle rest mass
ds	differential element of orbital arc length

$d^3\vec{P}$	element of volume in canonical momentum space
$d^3\vec{p}$	element of volume in mechanical momentum space
\vec{P}	canonical momentum vector

GEORGE C. MARSHALL SPACE FLIGHT CENTER

MTP-RP-64-1

DISTRIBUTION OF UNBOUND CHARGED PARTICLES
IN THE STATIC MAGNETIC FIELD OF A DIPOLE

by Arthur D. Prescott

SUMMARY

In this paper, Störmer's theory is summarized and the behavior of the allowed and forbidden regions with varying particle impact parameter is presented. Liouville's theorem is applied to the static magnetic field and the particle distribution is assumed to be in equilibrium over time. With these assumptions, the distribution function of particles in phase space at any given point (r, θ, ϕ) in a dipole field is determined, given the isotropic distribution at infinity. If an isotropic angular distribution at infinity is assumed, we find we can determine the allowed directions for particle motion at point (r, θ, ϕ) by mapping the point into the allowed and forbidden regions in Störmer space, via the Störmer transformation, at a particular particle impact parameter. The properties of the totally and partially shielded regions are then enumerated. Once the totally and partially shielded regions are established we find we can determine the momentum cutout in momentum space at point (r, θ, ϕ) by mapping the point into the total, partial, and unshielded regions in Störmer space with particle momentum as a variable. These methods are then used to find the proton flux ratio at points on the surface of a spherical spaceship as a function of particle kinetic energy. It is assumed that the spaceship offers no material shielding to the impinging particles. It is shown that the shielding effectiveness of the magnetic field depends strongly upon the shape of the volume to be shielded.

Finally the Störmer theory is extended to the finite current loop, and expressions for the allowed directions for particle motion and the momentum cutout at any point in the field are derived. The shape of the totally and partially shielded regions as a function of particle energy is studied and we find that the partially shielded region provides protection in the high energy regime where the totally shielded region is effectively nonexistent.

I. INTRODUCTION

For many years the motion of charged particles in the earth's magnetic field has been studied. Störmer studied the motion of charged particles in an infinitesimal dipole field. He numerically integrated the equations of motion to study special families of orbits and did the original research on the allowed and forbidden regions for particle motion. His work explained many of the interesting features of the aurorae and is presented in his book [2]. In 1933, Lemaitre and Vallarta refined Störmer's theory and studied envelopes of families of bound orbits adding additional information concerning the allowed unbound orbits through a given point in the field. Their work is summarized in Ref. [4]. Alfvén [12] added many original contributions and studied unbound particle orbits in the regime where the particle magnetic moment is essentially a constant of the motion. Chapman and Ferraro [13] postulated the existence of an equatorial ring current during a magnetic storm and Trieman [14], Ray [15], and others [16, 17] studied its effect upon the cosmic ray cutoffs on the earth. Quenby and Webber [18] took into account the higher order nondipole terms of the internal field of the earth and recalculated the cosmic ray cutoffs on the earth's surface. Lüst [19], Jory [20], and Kelsall [21] numerically integrated the equations of motion to determine the impact zones of solar cosmic ray particles upon the surface of the earth.

The discovery in 1961 of superconductors with higher critical fields and higher critical current densities awakened new interest in the possibility of the shielding of space vehicles with high magnetic fields generated by large currents flowing indefinitely in superconducting materials. The

magnetostatic field generated by the circulating currents would provide continuous protection against charged particles in space. Dow [22], Tooper and Kash [23], Brown [24], and Levy [11] have studied the shielding effectiveness of magnetostatic and electrostatic fields from a systems standpoint. Tooper and Kash concluded that an electrostatic system of concentric spheres was impractical. Dow showed that if ordinary conductors were used to carry the large currents, passive shielding is always superior. Levy considered a single current loop and concluded that magnetic shielding was superior weightwise for high particle energies (approximately 1 Bev). Urban [10] studied the allowed and forbidden regions of two coaxial current loops and also the magnetic quadrupole. Tooper and Kash initiated a study of the allowed and forbidden regions of the infinite solenoid. The study of these basic geometries is helpful in understanding the basic physical principles involved and is necessary to discover the interesting characteristics of each magnetic configuration. The 1960 International System of Units is used throughout this report.

II. STÖRMER THEORY SUMMARY

A. General Equations of Charged Particle Motion in a Static Magnetic and a Static Electric Field

The Lagrangian for charged particle motion in a time-independent magnetic and a time-independent electric field is:

$$L = T - U$$

where

$$T \equiv \frac{m\vec{v} \cdot \vec{v}}{2} \quad (\text{II-1})$$

and

$$U \equiv -q\vec{A} \cdot \vec{v} + q\phi_E \quad (\text{II-2})$$

The quantity $-q\vec{A} \cdot \vec{v} + q\phi_E$ is the generalized potential for charged particle motion in a static magnetic and electric field. Employing spherical coordinates (r, θ, ϕ) , and assuming the magnetic vector potential and the electrostatic potential are functions of r and θ only, the Euler-Lagrange equation provides two equations of motion and a first integral of motion corresponding to the cyclic coordinate ϕ :

$$\begin{aligned}
& m\ddot{r} - m r \dot{\theta}^2 - m r \sin^2 \theta \dot{\phi}^2 - q \sin \theta \dot{\phi} A_{\phi}(r, \theta) - q r \sin \theta \ddot{\phi} \frac{\partial A_{\phi}(r, \theta)}{\partial r} \\
& + q \frac{\partial \phi_E(r, \theta)}{\partial r} = 0
\end{aligned} \tag{II-3}$$

$$\begin{aligned}
& m r^2 \ddot{\theta} + 2 m r \dot{r} \dot{\theta} - m r^2 \sin \theta \cos \theta \dot{\phi}^2 - q r \cos \theta \ddot{\phi} A_{\phi}(r, \theta) \\
& - q r \sin \theta \ddot{\phi} \frac{\partial A_{\phi}(r, \theta)}{\partial \theta} + q \frac{\partial \phi_E(r, \theta)}{\partial \theta} = 0
\end{aligned} \tag{II-4}$$

$$m r^2 \sin^2 \theta \dot{\phi} + q r \sin \theta A_{\phi}(r, \theta) = P_{\phi} = \text{constant of the motion} \tag{II-5}$$

Since the Hamiltonian is independent of time [1], it is a constant of the motion:

$$H = T + q\phi_E = \text{constant of the motion}$$

B. Charged Particle Motion in a Steady State Dipole Magnetic Field

In a static magnetic field, the Lorentz force

$$\vec{F} = q [\vec{E} + \vec{v} \times \vec{B}]$$

is perpendicular to the velocity vector during the motion, for $\vec{E} = 0$. As a result, the speed of the particle or the kinetic energy of the particle is a constant of the motion. Rewriting Eq. (II-5) and dividing by the magnitude of the mechanical momentum, mv , we obtain

$$\frac{v_{\phi}}{v} + \frac{q A_{\phi}}{p} = \frac{P_{\phi}}{p r \sin \theta} \tag{II-6}$$

if

$$Q \equiv - \frac{v_{\phi}}{v} \equiv \sin \psi \tag{II-7}$$

$$2\gamma \equiv - \frac{P_{\phi}}{p} \tag{II-8}$$

(II-6) becomes

$$Q = \frac{qA_\phi}{p} + \frac{2\gamma}{r \sin \theta} \quad (II-9)$$

For an infinitesimal dipole:

$$\vec{A} = \frac{\vec{M} \times \vec{r}}{4\pi r^3}$$

If the dipole is orientated along the z-axis (Fig. 1) then $A_r = A_\theta = 0$,

$$A_\phi = \frac{M \sin \theta}{4\pi r^2} \quad (II-10)$$

Substituting Eq. (II-10) into Eq. (II-9):

$$Q = \frac{qM}{4\pi p} \frac{\sin \theta}{r^2} + \frac{2\gamma}{r \sin \theta}$$

If

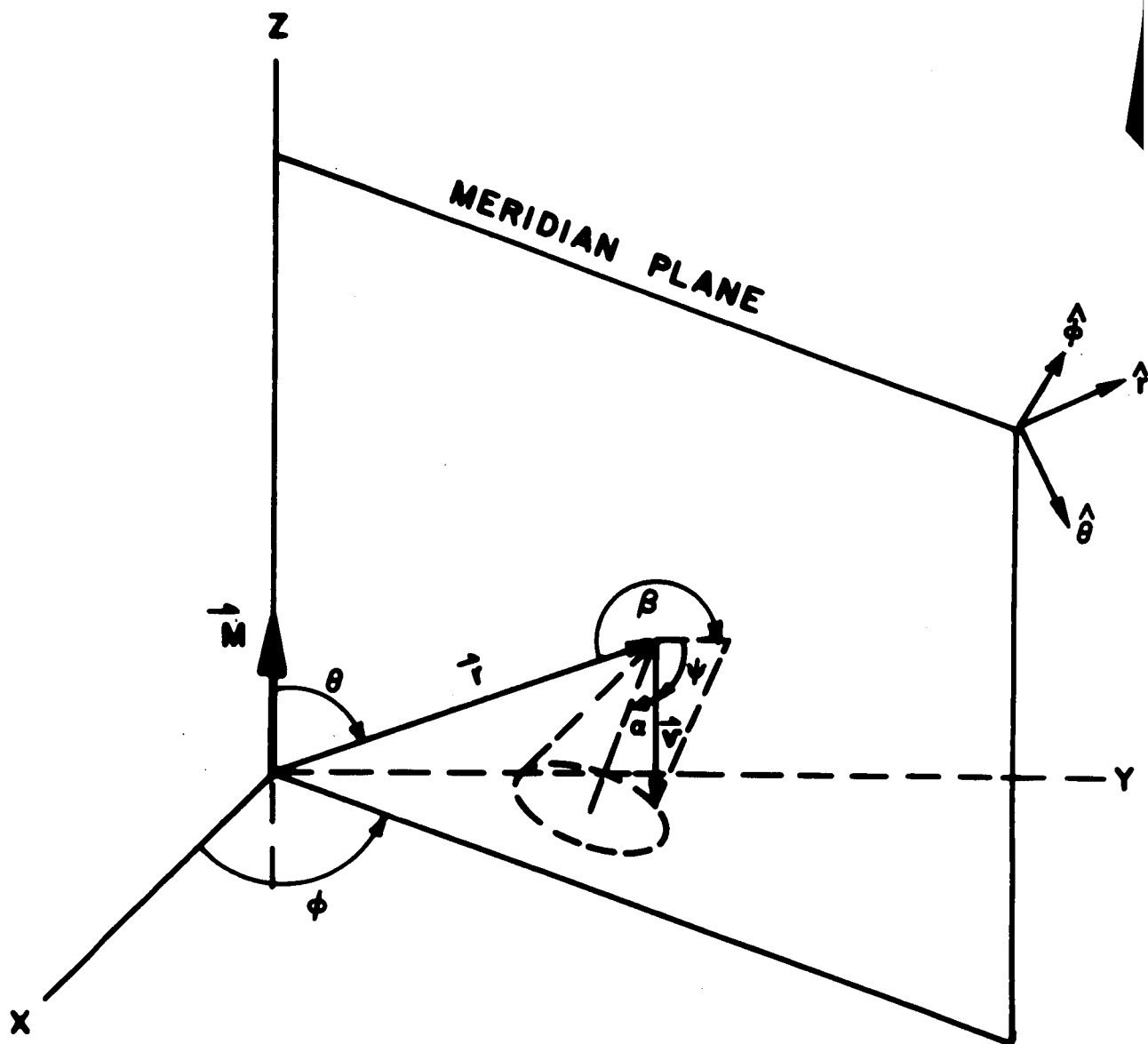
$$C_{st}^2 \equiv \frac{qM}{4\pi p} \quad (II-11)$$

then

$$Q = C_{st}^2 \frac{\sin \theta}{r^2} + \frac{2\gamma}{r \sin \theta} \quad (II-12)$$

The angle ψ is the angle the velocity vector makes with the meridian plane or $\sin \psi = -\hat{v} \cdot \hat{v}_\phi$.

If the canonical momentum component P_ϕ , a constant of the motion, is evaluated at infinity, $A_\phi \rightarrow 0$ and -2γ becomes the impact parameter. For a particle whose velocity vector lies in the equatorial plane the impact parameter is the closest distance of approach to the z-axis with the magnetic field absent. In general, -2γ is the ratio of the particle angular momentum about the dipole axis to the total linear momentum at infinity, and is a constant of the motion. To an observer traveling with a group of monodirectional particles impinging upon the dipole, the sign of the



$$v_r = -v \sin \alpha \cos \beta$$

$$v_\theta = -v \sin \alpha \sin \beta$$

$$v_\phi = -v \cos \alpha$$

Fig. I-REFERENCE COORDINATE SYSTEM

impact parameter distinguishes between those particles passing to the left and the right of the dipole, assuming the field is absent. The Störmer radius, C_{st} , has dimensions of length and for bounded motion is the radius of a particle with charge q and a momentum p moving in a circle in the equatorial plane of a dipole of strength M . The unbounded orbit in the equatorial plane with $\bar{\gamma} = -1.0$ is asymptotic to this bound orbit. However, we shall be concerned only with unbounded motion and the Störmer radius is considered a lumped parameter. Since the magnetic field simply changes the direction of motion, a particle originating "at infinity" returns to infinity. Reducing the right side of Eq. (II-12) to a non dimensional form by introducing the non-dimensional parameters

$$\bar{\gamma} \equiv \frac{\gamma}{C_{st}} \quad (II-13)$$

$$\rho \equiv \frac{r}{C_{st}} \quad (II-14)$$

we obtain the familiar Störmer equation [2]:

$$Q = \sin \psi = \frac{\sin \theta}{\rho^2} + \frac{2\bar{\gamma}}{\rho \sin \theta} \quad (II-15)$$

Since $Q \equiv -v\phi/v$, particle motion is restricted to those regions such that $-1.0 \leq Q \leq 1.0$. Solving Eq. (II-15) for ρ :

$$\rho = \frac{\sin^2 \theta}{-\bar{\gamma} \pm \sqrt{\bar{\gamma}^2 + Q \sin^3 \theta}} \quad (II-16)$$

The restrictions that ρ remain positive and real places restrictions on the parameters $\bar{\gamma}$ and Q , i.e.

$$\rho_0 = -\frac{\sin^2 \theta}{2\bar{\gamma}} \quad \left\{ \begin{array}{l} \bar{\gamma} < 0 \\ Q = 0 \end{array} \right\} \quad (II-17)$$

$$\rho_1 = \frac{\sin^2 \theta}{-\bar{\gamma} + \sqrt{\bar{\gamma}^2 + Q \sin^3 \theta}} \quad \begin{cases} Q > 0 \\ \text{no restrictions} \\ \text{on } \bar{\gamma} \end{cases} \quad (\text{II-18})$$

$$\rho_2 = \frac{\sin^2 \theta}{-\bar{\gamma} + \sqrt{\bar{\gamma}^2 + Q \sin^3 \theta}} \quad \begin{cases} Q < 0 \\ Q \geq \bar{\gamma}^2 / \sin^3 \theta \\ \bar{\gamma} < 0 \end{cases} \quad (\text{II-19})$$

$$\rho_3 = \frac{\sin^2 \theta}{-\bar{\gamma} - \sqrt{\bar{\gamma}^2 + Q \sin^3 \theta}} \quad \begin{cases} Q < 0 \\ Q \geq \bar{\gamma}^2 / \sin^3 \theta \\ \bar{\gamma} < 0 \end{cases} \quad (\text{II-20})$$

Using $\rho(-1, 1)$ as a shorthand notation for " $\rho(\bar{\gamma}, Q)$ with $\bar{\gamma} = -1.0$ and $Q = 1.0$," $\rho_1(\bar{\gamma}, 1)$ defines an inner forbidden region with $Q = 1.0$ on its outer boundary. Q is greater than 1.0 within this region. For $-\infty \leq \bar{\gamma} < 0$, $\rho_2(\bar{\gamma}, -1)$ and $\rho_3(\bar{\gamma}, -1)$ define an outer forbidden region with $Q = -1.0$ on its outer boundaries. Q is less than -1.0 within this region and particle motion is forbidden. The forbidden and allowed regions are plotted in Fig. 2 for three values of $\bar{\gamma}$. For $\bar{\gamma} \leq -1.0$, $\rho_1(\bar{\gamma}, -1)$ and $\rho_2(\bar{\gamma}, -1)$ define an inner allowed region; and an outer allowed region extends from $\rho_3(\bar{\gamma}, -1)$ to infinity. The outer forbidden region exists for $-\infty \leq \bar{\gamma} < 0$ and disappears at $\bar{\gamma} = 0$. For $\bar{\gamma}$ slightly greater than zero, the inner forbidden region sends up small appendages on either side of the dipole axis. Thus the z-axis is in an allowed region only for $\bar{\gamma} = 0$, and the origin is accessible only to particles such that $-1.0 < \bar{\gamma} \leq 0$. Since Eq. (II-16) is independent of ϕ , the forbidden regions are rotationally symmetric about the z-axis. The behavior of the forbidden regions as $\bar{\gamma}$ varies is described in a later section. Throughout this section, the particles are assumed to move at non-relativistic velocities. However, Eq. (II-12) is valid at relativistic velocities and all previous statements are valid if we use the relativistic expressions for the momentum and kinetic energy:

$$p = \frac{[T^2 + 2Tmc^2]^{\frac{1}{2}}}{c} \quad (\text{II-21})$$

$$T = [p^2 c^2 + m^2 c^4]^{\frac{1}{2}} - mc^2 \quad (\text{II-22})$$

The particle speed is a constant of the motion, since the Lorentz force is perpendicular to the velocity vector for $\vec{E} = 0$. Relativistic equations of motion are derived in Appendix I.

C. Störmer Space and Related Topics

The Störmer transformation (Eq. II-14) is a transformation which connects the radial coordinate r with kinetic energy, T . The distribution function of particles in phase space $f(r, \theta, \phi, T, \alpha, \beta) \rightarrow f(\rho, \theta, \phi, \alpha, \beta)$. Thus, instead of considering orbits of particles of different energies in a fixed field, we may find the orbit of a particle with a given energy in Störmer space, (ρ, θ, ϕ) . Then by a linear change of scale, we know the orbits for particles of any other energy with the same injection point and direction of injection into the field.

The advantage of studying the forbidden and allowed regions in Störmer space is as follows. The equations

$$\rho_E = r_E / C_{st}(T) \quad (\text{II-23})$$

$$\rho = \frac{\sin^2 \theta}{1 + \sqrt{1 \pm \sin^3 \theta}} \quad (\text{II-24})$$

define the radius of the earth (a sphere) and the inner and outer forbidden regions in Störmer space for $\bar{\gamma} = -1.0$. Equation (II-24) is invariant with particle energy, while the earth's radius changes according to Eq. (II-23). ρ is nondimensional and therefore the scale has no units. In real space the equations become

$$r_E = \text{constant} \quad (\text{II-25})$$

$$r = C_{st} \left[\frac{\sin^2 \theta}{1 + \sqrt{1 \pm \sin^3 \theta}} \right]. \quad (\text{II-26})$$

In real space (r, θ, ϕ) , the radius of the earth is fixed and the forbidden regions change with particle energy according to Eq. (II-26).

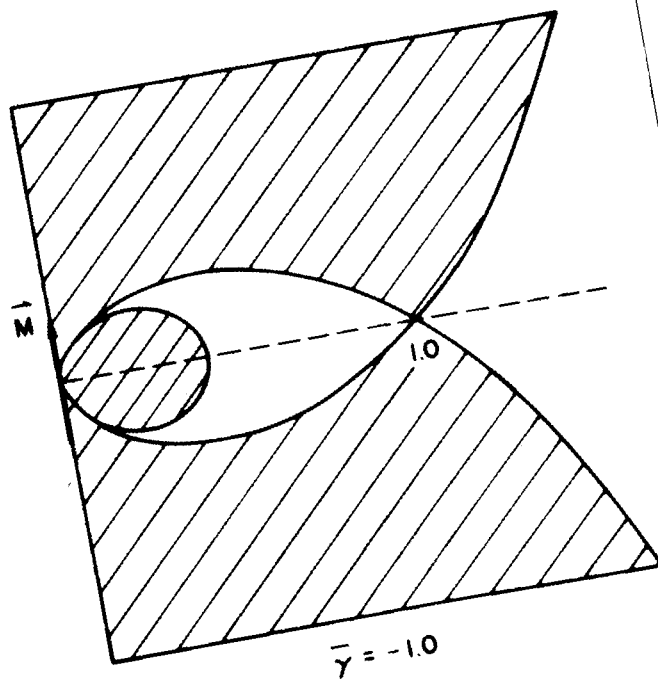
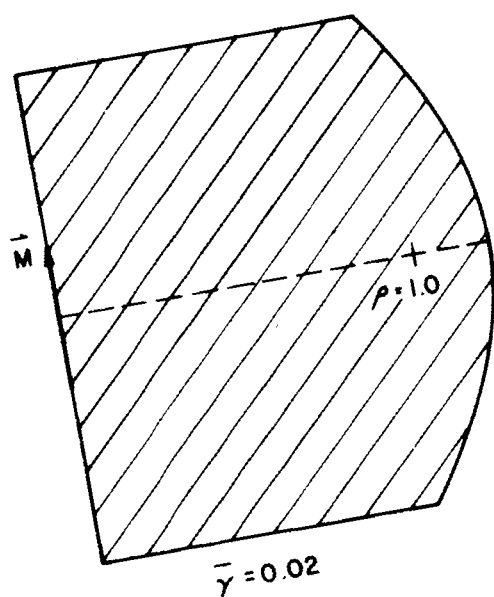
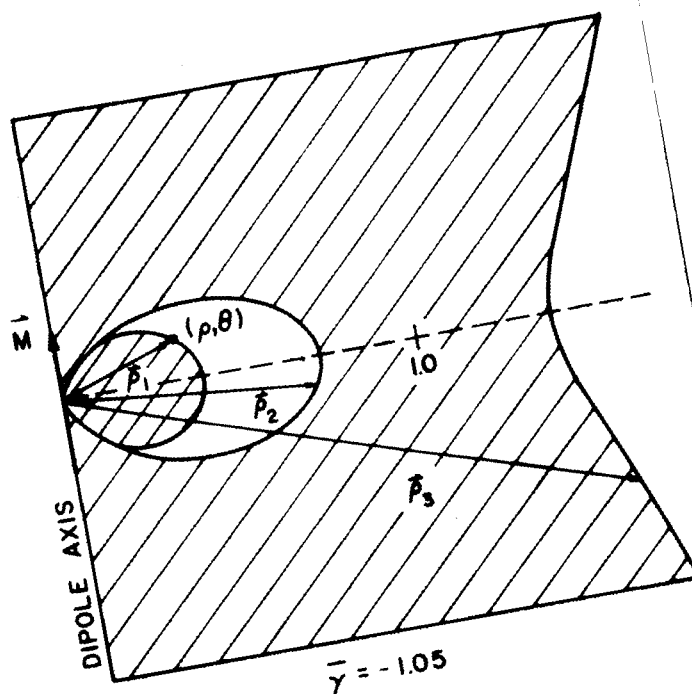
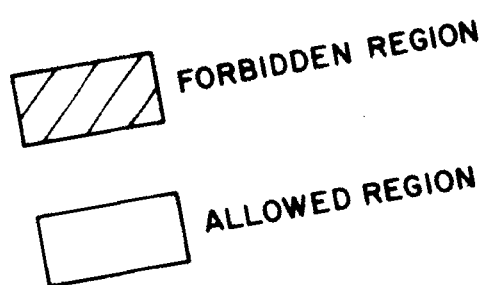


Fig.2-ALLOWED AND FORBIDDEN REGIONS FOR THREE SELECT VALUES OF $\bar{\gamma}$ IN THE (p, θ) PLANE.

The scale has units of length or units of C_{st} . C_{st} is a given number of meters depending, in a fixed field, upon the particle's charge and momentum.

Figures 3 and 4 show C_{st} for electrons and protons as a function of particle energy in different dipole moment magnetic fields. At nonrelativistic energies, in a fixed field:

$$\frac{C_{st}(e^-)}{C_{st}(p^+)} = \left[\frac{m_{p^+}}{m_{e^-}} \right]^{\frac{1}{4}} \left[\frac{T_{p^+}}{T_{e^-}} \right]^{\frac{1}{4}}.$$

As the particle energy increases without bounds:

$$\frac{C_{st}(e^-)}{C_{st}(p^+)} \rightarrow 1.0.$$

Thus the electrons in a low-energy monoenergetic beam of electrons and protons are deflected by the magnetic field sooner than the protons. In real space, at nonrelativistic energies, the forbidden regions in a dipole field for protons should be scaled by a factor 6.6 to arrive at the forbidden regions for the electrons. At relativistic energies, the field does not distinguish between electrons and protons, that is, it is equally effective as a shield.

From a mathematical standpoint, the Störmer equation (Eq. II-15) is a necessary condition that a particle must satisfy to exist at a given point. Sufficiency is guaranteed by solving all of the equations of motion simultaneously. The ρ curves shown in Fig. 2 are the outer boundaries of the allowed orbits projected upon the meridian plane. Störmer showed that particle motion could be broken into two coupled motions — motion of the particle within the meridian plane and motion of the meridian plane about the dipole axis. Equation (II-9) corresponding to the cyclic coordinate ϕ determines the angle the velocity vector makes with the meridian plane as a function of position within the meridian plane, as the particle impact parameter varies.

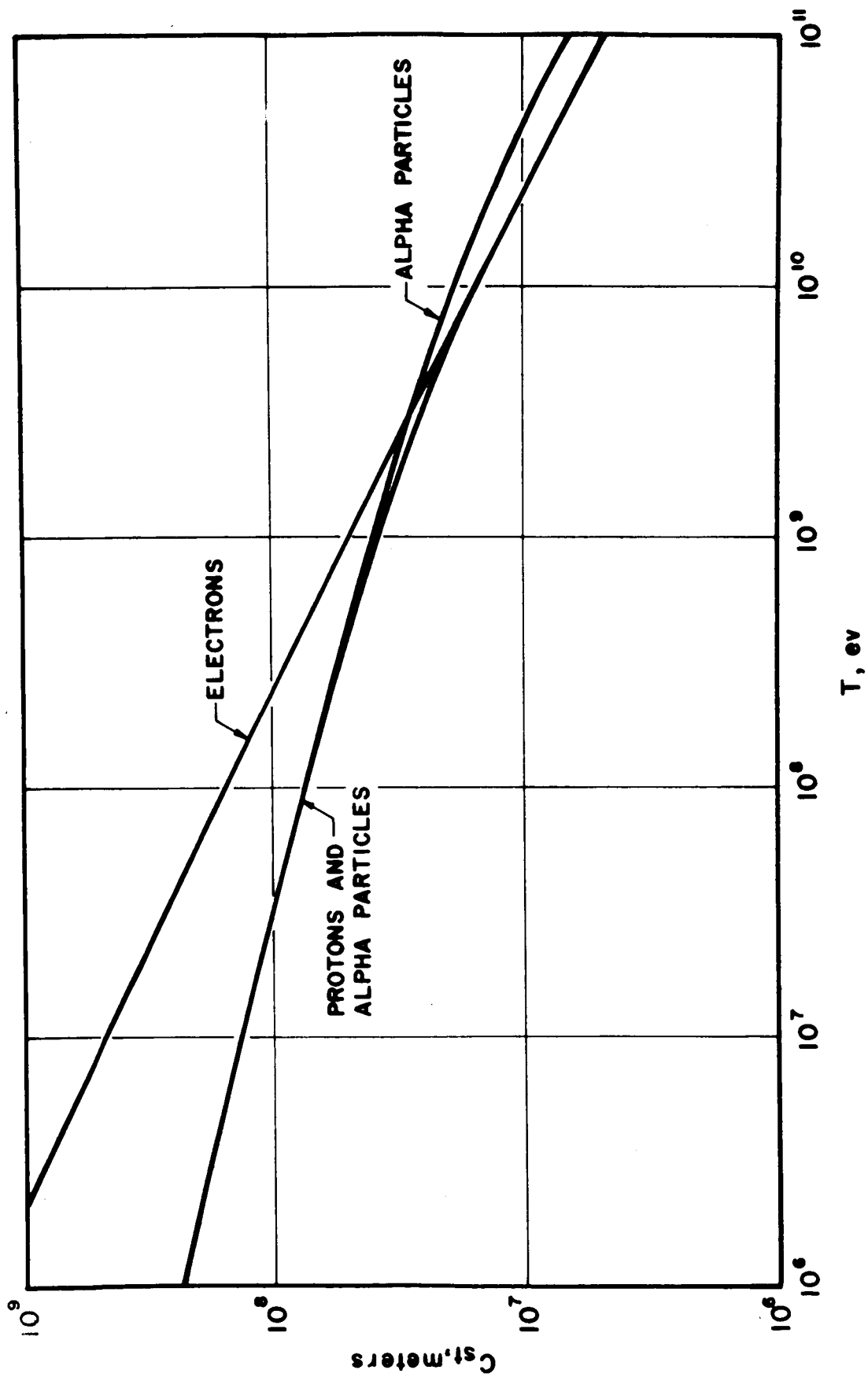


Fig. 3-PARTICLE STÖRMER RADIUS FOR PROTONS, ELECTRONS, AND ALPHA PARTICLES IN THE EARTH'S MAGNETIC FIELD, $M = 1.01788 \times 10^{17}$ weber-meters, vs KINETIC ENERGY.

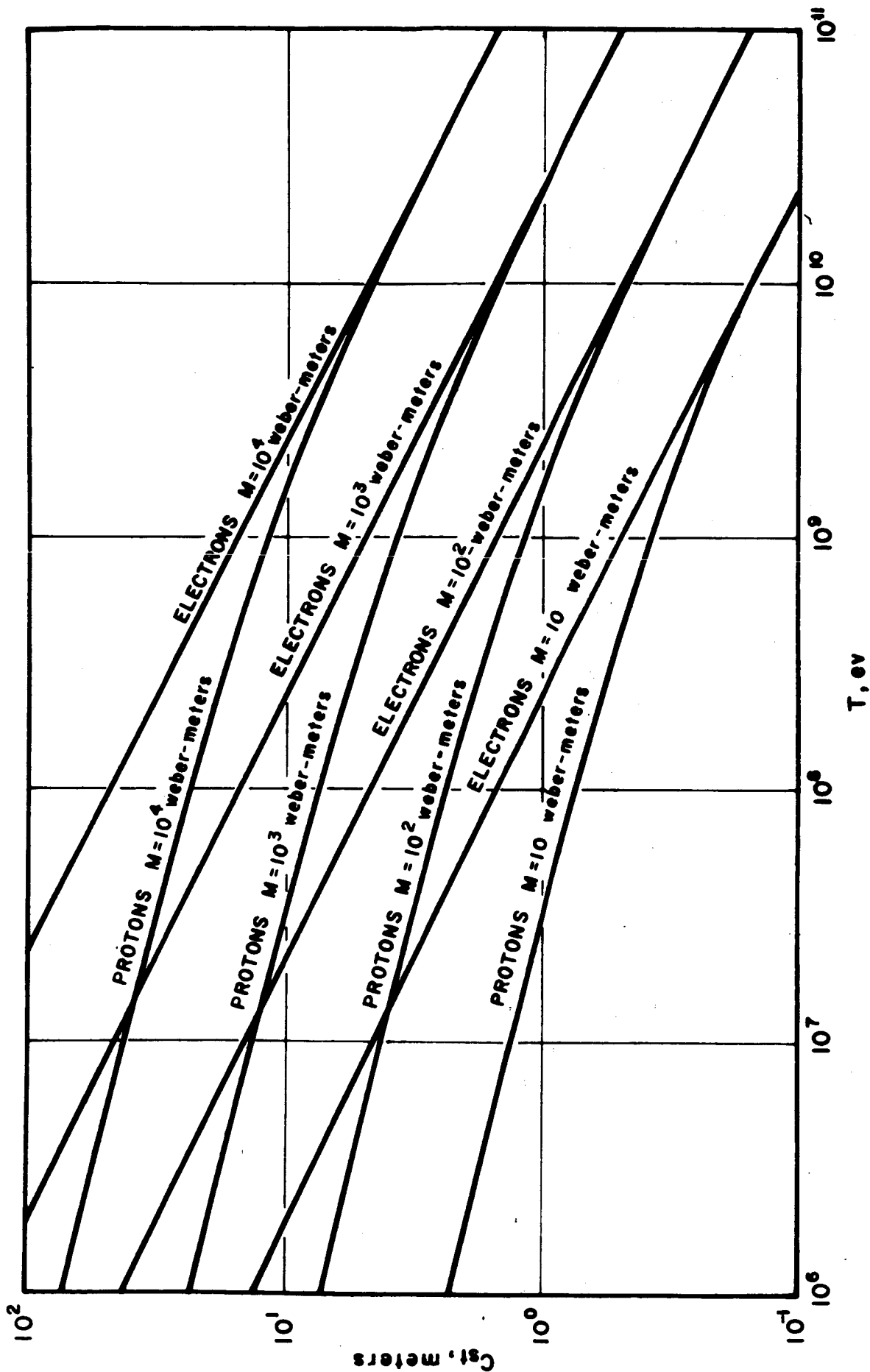


Fig. 4-PARTICLE STÖRMER RADIUS FOR PROTONS AND ELECTRONS vs. KINETIC ENERGY, WITH MAGNETIC DIPOLE MOMENT AS A PARAMETER.

III. PARTICLE DISTRIBUTION IN THE MAGNETIC FIELD OF AN INFINITESIMAL DIPOLE

A. Liouville's Theorem and Its Application to a Static Magnetic Field

Consider a swarm of n particles in a $2n$ phase space (q_i, P_i) , $i = 1, \dots, n$. At a particular time t assign a number to each point to represent the density of particles per unit volume of real space per unit volume of momentum space. Define a scalar point function $f(q_i, P_i, t)^*$ with the aforementioned units to give the function relationship between the numbers. Then, taking the total derivative:

$$\frac{df}{dt} = \sum \left[\frac{\partial f}{\partial q_i} \dot{q}_i + \frac{\partial f}{\partial P_i} \dot{P}_i \right] + \frac{\partial f}{\partial t} . \quad (\text{III-1})$$

Applying Liouville's theorem and assuming the particle density is low enough so that the particles do not collide:

$$\frac{df}{dt} = 0 \quad (\text{III-2})$$

$\frac{df}{dt} = 0$ is also the mathematical statement of the collisionless, no radiation loss, Boltzman equation.

Assuming the particle distribution is in equilibrium over time:

$$\frac{\partial f}{\partial t} = 0$$

If the generalized coordinates and generalized momenta satisfy Hamilton's canonical equations of motion:

$$\frac{\partial H}{\partial P_i} = \dot{q}_i : \frac{\partial H}{\partial q_i} = -\dot{P}_i$$

* In this paper, small parentheses are used to indicate functional dependence within an equation.

then

$$\sum_i \left[\frac{\partial f}{\partial q_i} \frac{\partial H}{\partial P_i} - \frac{\partial f}{\partial P_i} \frac{\partial H}{\partial q_i} \right] = 0 \quad (\text{III-3})$$

or

$$[f, H] = 0 \quad (\text{III-4})$$

where the brackets of Eq. (III-4) are the Poisson brackets. Consequently, (Ref. 1) f is a constant of the motion along a trajectory generated by the Hamiltonian in phase space. Equation (III-2) is the mathematical statement of Liouville's theorem. If the nature of the force field is known, Liouville's theorem will furnish information about the particle distribution in the field without solving for the trajectories of individual particles and recording the number of particles in each volume element with a given energy and direction over a large time interval.

Since the equations of motion of a charged particle moving in a static magnetic field can be derived using Hamilton's canonical equations of motion (Appendix I), and assuming the particle distribution is in equilibrium over time, and applying Liouville's theorem, then the distribution function f is a constant of the motion along a trajectory through phase space.

Consider a six-dimensional space composed of three position coordinates and three canonical momentum coordinates. For application to a static magnetic and static electric field, it would be more convenient to apply Liouville's theorem to a six-dimensional space composed of three position coordinates and three mechanical momentum coordinates. We will show that the Jacobian

$$\frac{\partial (q_1, q_2, q_3, P_1, P_2, P_3)}{\partial (q_1, q_2, q_3, p_1, p_2, p_3)} = 1 \quad (\text{III-5})$$

under the transformation

$$\left. \begin{aligned} q_i &= q'_i \\ P_i &= p'_i + qh_i A_i(q_i) \end{aligned} \right\} \quad i = 1, 2, 3 \quad (\text{III-6})$$

where A_i is the i^{th} component of the magnetic vector potential, P_i is the canonical momentum and p'_i is the mechanical momentum. Writing out this sixth order determinant and observing that

$$\left. \begin{aligned} \frac{\partial P_i}{\partial p'_j} &= \delta_{ij} ; \frac{\partial q_i}{\partial q'_j} = \delta_{ij} ; \frac{\partial q_i}{\partial p'_i} = \frac{\partial q_i}{\partial q_j} \frac{\partial q_j}{\partial p'_i} = 0 \\ \frac{\partial P_i}{\partial q'_j} &= \frac{\partial [qh_i A_i]}{\partial q_j} = q \left[\frac{\partial A_i}{\partial q_j} + A_i \frac{\partial h_i}{\partial q_j} \right] \equiv B_{ij} \end{aligned} \right\} \begin{aligned} i &= 1, 2, 3 \\ j &= 1, 2, 3 \end{aligned}$$

the determinant becomes

$$\begin{vmatrix} 1 & 0 & 0 & B_{11} & B_{21} & B_{31} \\ 0 & 1 & 0 & B_{12} & B_{22} & B_{32} \\ 0 & 0 & 1 & B_{13} & B_{23} & B_{33} \\ 0 & 0 & 0 & 1 & 0 & 0 \\ 0 & 0 & 0 & 0 & 1 & 0 \\ 0 & 0 & 0 & 0 & 0 & 1 \end{vmatrix}$$

and when expanded, the determinant is equal to one. This was first shown by Swann [3] who noted that Eq. (III-5) is valid even when a static electric field is present; the canonical momenta are still given by Eq. (III-6). Thus we may integrate over mechanical momentum space instead of canonical momentum space. Henceforth, the word momentum will refer to the mechanical momentum.

B. Monoenergetic, Isotropic, Homogeneous Distribution at an Infinite Distance Away from the Dipole

Let $f(\vec{r}, \vec{P})$ be the distribution function referred to in Liouville's theorem where $q_i, P_i, i = 1, 2, 3$ are the components of \vec{r} and \vec{P} , respectively. The mechanical momentum vector \vec{p} may be defined by giving the kinetic energy of the particle and the direction of motion:

$$f(\vec{r}, \vec{p}) d^3\vec{p} = f(\vec{r}, T, \hat{\Omega}) dT d\Omega. \quad (\text{III-7})$$

Since the speed v is a constant of the motion, $vf(\vec{r}, \vec{P})$ is conserved, by Liouville's theorem, along a trajectory in phase space which connects two points in real space. Of course, a given point in real space may be intersected by more than one trajectory through phase space, but Liouville's theorem states that $f(\vec{r}, \vec{P})$ is constant and has the same value along a given trajectory and its projection in real space. Furthermore, trajectories cannot intersect in phase space. Liouville's theorem together with the constants of motion determine the distribution functions which are constant at two points in real space connected by a trajectory through phase space. The equations of motion provide us with the coordinates of the two points along with the limits on the integrals. For an isotropic distribution, it is unnecessary to determine the direction dependence of the particle orbit explicitly. Flux is defined by the integral:

$$\Phi(\vec{r}) = \int_{\Omega} \int_T vf(\vec{r}, T, \hat{\Omega}) dT d\Omega. \quad (\text{III-8})$$

From the last section:

$$f(\vec{r}, \vec{P}) d^3\vec{P} \equiv f(\vec{r}, \vec{p}) d^3\vec{p} = f(\vec{r}, T, \hat{\Omega}) dT d\Omega.$$

Henceforth, we shall drop the differentials when referring to the distribution function.

The flux "at infinity" is

$$\Phi(\vec{r}_\infty) = \int_{\Omega_\infty} \int_{T_\infty} v f(\vec{r}, T, \hat{\Omega}) dT d\Omega \quad (\text{III-9})$$

$$\frac{\Phi(\vec{r})}{\Phi(\vec{r}_\infty)} = \frac{\int_{\Omega} \int_T v f(\vec{r}, T, \hat{\Omega}) dT d\Omega}{\int_{\Omega_\infty} \int_T v f(\vec{r}, T, \hat{\Omega})_\infty dT d\Omega} \quad (\text{III-10})$$

Invoking Liouville's theorem:

$$v f(\vec{r}, T, \hat{\Omega}) = v f(\vec{r}, T, \hat{\Omega})_\infty \quad (\text{III-11})$$

For a monoenergetic, isotropic, homogeneous source at infinity of energy T_0 :

$$v f(\vec{r}, T, \hat{\Omega})_\infty = \delta [T - T_0(\vec{r}_\infty)] \quad (\text{III-12})$$

Equation (III-10) becomes

$$\frac{\Phi(\vec{r})}{\Phi(\vec{r}_\infty)} = \frac{\int_{\Omega} \int_T \delta [T - T_0(\vec{r}_\infty)] dT d\Omega}{\int_{\Omega_\infty} \int_T \delta [T - T_0(\vec{r}_\infty)] dT d\Omega} \quad (\text{III-13})$$

$$d\Omega \equiv \sin \alpha d\alpha d\beta \quad (\text{III-14})$$

$$\frac{\Phi(\vec{r})}{\Phi(\vec{r}_\infty)} = \frac{2\pi}{4\pi} \int_{\alpha_1(\vec{r})}^{\alpha_2(\vec{r})} \sin \alpha d\alpha = \frac{1}{2} [\cos \alpha_1 - \cos \alpha_2] \quad (\text{III-15})$$

Referring to Fig. 1, ψ is the angle between the velocity vector and the meridian plane; and α is its complement. The particle distribution $vf(\vec{r}, T, \hat{\Omega})$ is symmetric in angle β , since Eq. (II-15) is invariant to rotation of \vec{v} about the perpendicular to the meridian plane. Equation (II-15) defines a cone of directions with half angle α :

$$\cos \alpha = \sin \psi \equiv Q = \frac{\sin \theta}{\rho^2} + \frac{2\bar{\gamma}}{\rho \sin \theta} \quad (\text{III-16})$$

and Eq. (III-15) becomes:

$$\frac{\Phi(\vec{r})}{\Phi(\vec{r}_\infty)} = \frac{1}{2} [Q_1(\vec{r}) - Q_2(\vec{r})] \quad (\text{III-17})$$

To determine Q_1 and Q_2 , we must examine the expansion and contraction of the forbidden regions, defined by Eqs. (II-18), (II-19), and (II-20), with varying impact parameter.

C. Dependence of the Forbidden Regions on Impact Parameter

An isotropic distribution at \vec{r}_∞ implies that the impact parameter of a particle may have values $-\infty \leq -2\bar{\gamma} \leq \infty$ or $-\infty \leq -2\bar{\gamma} \leq \infty$, $T > 0$. Differentiating Eqs. (II-18), (II-19), and (II-20):

$$\frac{\partial \rho_1}{\partial \bar{\gamma}} = \frac{1}{Q \sin \theta} + \frac{\bar{\gamma}}{Q \sin \theta \sqrt{\bar{\gamma}^2 + Q \sin^3 \theta}} \quad (\text{III-18})$$

$$\frac{\partial \rho_2}{\partial \bar{\gamma}} = \frac{1}{Q \sin \theta} + \frac{\bar{\gamma}}{Q \sin \theta \sqrt{\bar{\gamma}^2 + Q \sin^3 \theta}} \quad (\text{III-19})$$

$$\frac{\partial \rho_3}{\partial \bar{\gamma}} = \frac{1}{Q \sin \theta} - \frac{\bar{\gamma}}{Q \sin \theta \sqrt{\bar{\gamma}^2 + Q \sin^3 \theta}} \quad (\text{III-20})$$

The inner forbidden region defined by $\rho_1(\bar{\gamma}, 1)$ is very small compared to the outer forbidden region defined by $\rho_2(\bar{\gamma}, -1)$ and $\rho_3(\bar{\gamma}, -1)$, for $\bar{\gamma} \ll -1.0$. As $\bar{\gamma} \rightarrow 0$ the inner forbidden region expands with respect to ρ and the outer forbidden region contracts. The outer forbidden region disappears at $\bar{\gamma} = 0$ while the inner forbidden region continues to expand as $\bar{\gamma}$ becomes more positive.

Given a point (r, θ, ϕ) , the equations

$$\rho = r/C_{st} \quad (\text{III-21})$$

$$Q = \frac{\sin \theta}{\rho^2} + \frac{2\bar{\gamma}}{\rho \sin \theta} \quad (\text{III-22})$$

define Q , given $\bar{\gamma}$ and C_{st} which is defined by Eq. (II-11). Consider the important case $\bar{\gamma} = -1.0$ shown in Fig. 5. In light of the preceding discussion, if the point falls within the inner forbidden region, it will forever be inaccessible to incoming particles regardless of their impact parameter, for the inner forbidden region expands as $\bar{\gamma}$ increases from -1.0 . As $\bar{\gamma}$ becomes slightly greater than -1.0 , point B will begin to see particles until for some $\bar{\gamma}$ ($Q = 1.0$) the inner forbidden region engulfs the point. For case C, as $\bar{\gamma}$ increases from -1.0 , the outer forbidden region will contract until point C falls on its boundary $Q = -1.0$. As $\bar{\gamma}$ continues to increase point C will continue to see particles with various Q until for some $\bar{\gamma}$ ($Q = 1.0$), the inner forbidden region will engulf the point.

To analyze case D, we shall have to consider the case $\bar{\gamma} < -1.0$. For some large negative $\bar{\gamma}$ ($Q = -1.0$), point D will fall on the boundary of the outer forbidden region. As $\bar{\gamma}$ increases from this value, the outer forbidden region will contract and point D will begin to see particles. Let $\bar{\gamma}$ continue to become more positive, then point D continues to see particles of various Q until for some $\bar{\gamma}$ ($Q = 1.0$) the inner forbidden region will engulf point D.

Thus, at a particular $\bar{\gamma}$, namely $\bar{\gamma} = \bar{\gamma}_c = -1.0$, points within the inner forbidden region will never subtend any solid angle to incoming particles. Points within the inner allowed region will subtend a solid angle ranging from slightly greater than 0 up to slightly less than 4π .

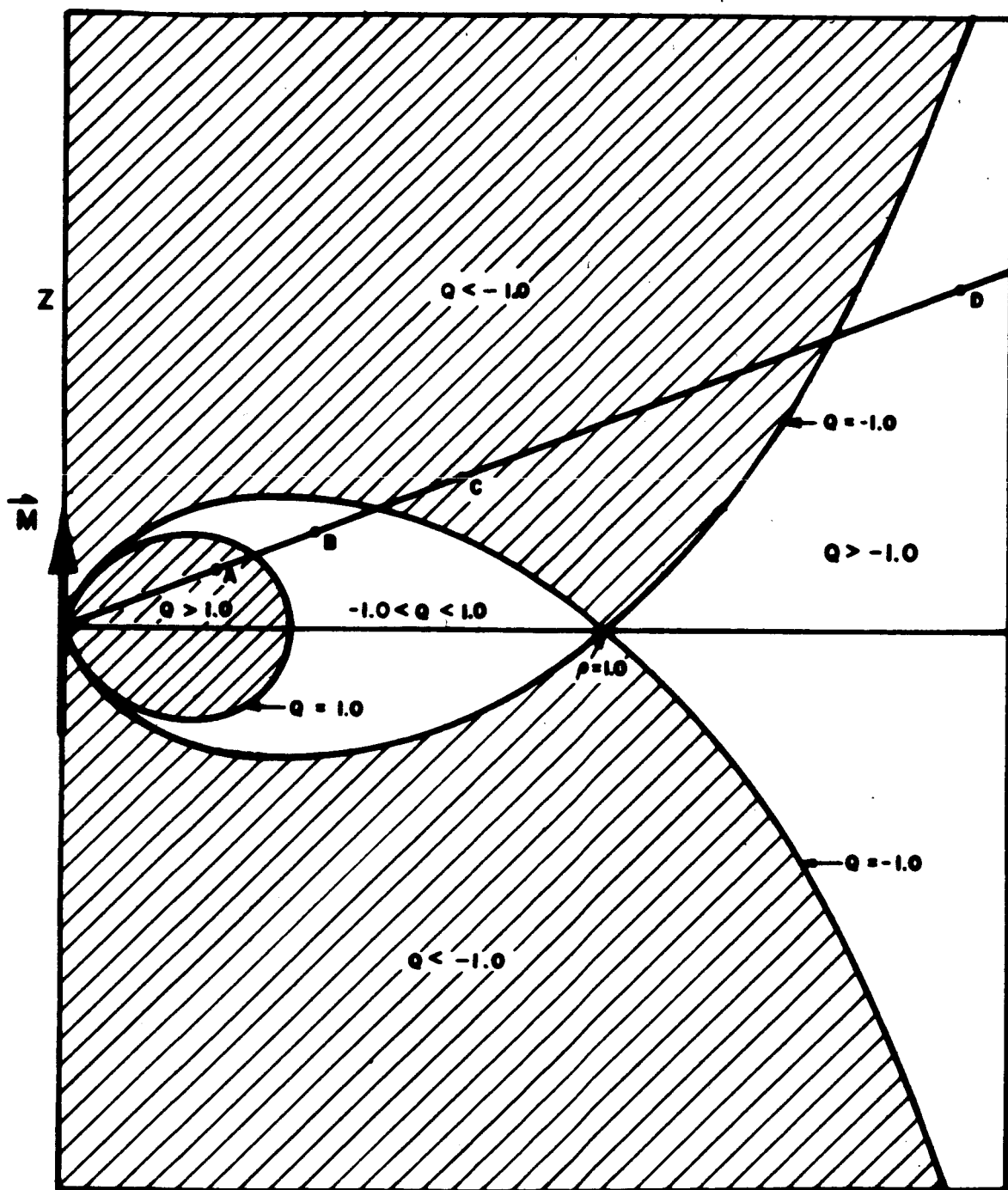


Fig.5-ALLOWED AND FORBIDDEN REGIONS IN THE (ρ, θ) PLANE FOR $\bar{\gamma} = -1.0$.

There will always be a range of impact parameters such that points within the outer forbidden and outer allowed region will subtend 4π solid angles to incoming particles, regardless of the distance from the dipole since $-\infty \leq 2\bar{\gamma} \leq \infty$. With Liouville's theorem in mind, at $\bar{\gamma} = \bar{\gamma}_c = -1.0$, points within the outer allowed and outer forbidden regions can be connected up to infinity in any direction by trajectories through phase space. Points within the inner allowed region can be connected up with infinity in certain directions. Points within the inner forbidden region can never be connected up to infinity by a trajectory through phase space. Thus the inner forbidden region is totally void of particles regardless of the particle distribution at infinity.

In any magnetic field whose outer forbidden region completely surrounds the inner forbidden region at some $\bar{\gamma} = \bar{\gamma}_c$, and whose forbidden regions behave in the same manner as the forbidden regions of the dipole field in the sense that one forbidden region expands while the other contracts with varying impact parameter, then the inner forbidden region at $\bar{\gamma} = \bar{\gamma}_c$ will always be completely void of particles regardless of the particle distribution at infinity. From Eq. (II-9), for $-\infty \leq 2\bar{\gamma} \leq \infty$, it appears that the forbidden regions in any magnetic field will behave in this manner if $A \propto 1/r^n$, $n \geq 2$.

We define Q_c as the value of Q computed from Eq. (III-22) with $\bar{\gamma} = \bar{\gamma}_c = -1.0$. $\cos^{-1} Q_c$ is the cone half angle of the allowed solid angle subtended at points within the inner allowed region.

$$Q_c = \frac{\sin \theta}{\rho^2} - \frac{2}{\rho \sin \theta} = C_{st}^2 \frac{\sin \theta}{r^2} - \frac{2C_{st}}{r \sin \theta} \quad (\text{III-23})$$

We can determine which of the four regions point (r, θ, ϕ) will be mapped into, under the Störmer transformation, by performing tests on Q_c and $\partial Q_c / \partial \rho$. The four regions have the following unique properties:

Inner forbidden region: $Q_c \geq 1.0$

Outer forbidden region: $Q_c \leq -1.0$

Inner allowed region: $-1.0 < Q_c < 1.0$ and $\partial Q_c / \partial \rho < 0$

Outer allowed region: $-1.0 < Q_c < 0$ and $\partial Q_c / \partial \rho > 0$

Given a point (r, θ, ϕ) and computing Q_c from Eq. (III-23) then:

$$\frac{\Phi(\vec{r})}{\Phi(\vec{r}_\infty)} = 0 \text{ if } Q_c \geq 1.0 \quad (\text{completely shielded region}) \quad (\text{III-24})$$

$$\frac{\Phi(\vec{r})}{\Phi(\vec{r}_\infty)} = 1 \quad \begin{cases} \text{if } Q_c \leq -1.0 & (\text{completely unshielded region}) \\ \text{if } -1.0 < Q_c < 0 \text{ and } \frac{\partial Q_c}{\partial \rho} > 0 \end{cases} \quad (\text{III-25})$$

$$\frac{\Phi(\vec{r})}{\Phi(\vec{r}_\infty)} = \frac{1}{2} [1 - Q_c] \text{ if } -1.0 < Q_c < 1.0 \text{ and } \frac{\partial Q_c}{\partial \rho} < 0$$

(partially shielded region) (III-26)

Figure 6 shows the totally shielded and partially shielded regions in the (ρ, θ) plane. The regions are rotationally symmetric about the dipole axis.

A refinement of the theory by Lemaitre and Vallarta predicts that certain directions are forbidden within the inner allowed region for $-1.0 < \gamma \leq -0.788541$ but our use of the Störmer theory will predict conservative results without resorting to numerical integration to determine bound orbits. Their theory, briefly, is as follows: orbits are not distinguished by the total energy such as orbits in a gravitational field. In Störmer space, a particle's orbit depends only upon its injection point and the direction that it is injected into the field (since the particle kinetic energy is a constant of the motion). Lemaitre and Vallarta have shown [4, 5, and 6] that bound orbits exist within the inner allowed region even when the outer forbidden region has opened up — allowing unbound particles from infinity to enter. These bound orbits are bounded by an inner periodic and an outer periodic orbit which coalesce as $\gamma \rightarrow -0.788541$. If a bound orbit passes through a point $\vec{\rho}$, that direction is forbidden to unbound particles and also to other bound particles following different orbits; for none of the trajectories in phase space can intersect in phase space. Since kinetic energy is a constant of the motion, this direction at $\vec{\rho}$ is forbidden

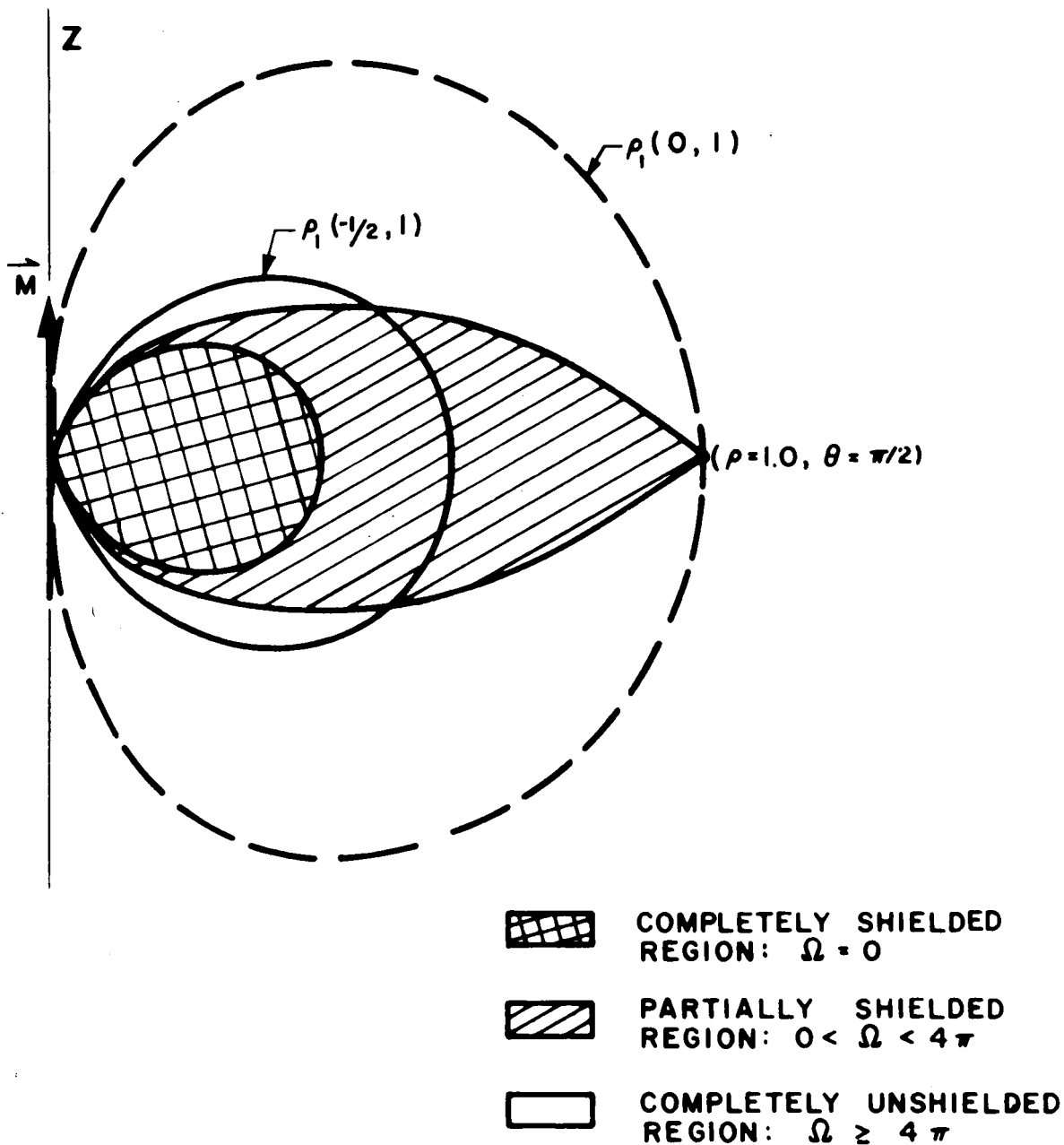


Fig.6-SHIELDED REGIONS OF AN INFINITESIMAL MAGNETIC DIPOLE FIELD IN THE (ρ, θ) PLANE.

to all unbound particles, regardless of their kinetic energy. Schremp [7] has shown that at points $\bar{\rho}$ within the inner allowed regions, an infinitesimal and/or a finite bundle of bound orbits may pass through $\bar{\rho}$. Thus infinitesimal or finite solid angles, or both, may be forbidden to unbound particles arriving at points (ρ, θ) within the inner allowed region.

We can also add further information to Fig. 6 about the range of impact parameters particles must have to exist in a region of the (ρ, θ) plane. Solving Eq. (III-22) for $2\bar{\gamma}$:

$$2\bar{\gamma} = \sin \theta \left[Q\rho - \frac{\sin \theta}{\rho} \right] \quad . \quad (\text{III-27})$$

Suppose we reverse our procedure and plot curves of constant $\bar{\gamma}$ with Q as a parameter. Let us divide the range of Q for allowed motion into two sub-intervals: $-1.0 \leq Q \leq 0$ and $0 < Q \leq 1.0$. For $-1.0 \leq Q \leq 0$, $\bar{\gamma}$ is negative and particles with negative impact parameters may exist anywhere within the (ρ, θ) plane except within the totally shielded region. For $0 < Q \leq 1.0$, setting $2\bar{\gamma} = 0$ in Eq. (III-27) provides the following information: inside the boundaries of the surface

$$\rho_1(0, Q) = \sqrt{\frac{\sin \theta}{Q}} \quad (\text{III-28})$$

particles with negative impact parameters may exist. Outside this surface, particles with positive impact parameters may exist. The surface $\rho_1(0, 1) = \sqrt{\sin \theta}$ is the smallest surface of these Q and $\bar{\gamma} = 0$ surfaces. Examining the entire interval $-1.0 \leq Q \leq 1.0$, $\rho_1(0, 1)$ defines a limiting surface. Inside this surface, only particles with negative impact parameters may exist. Outside this surface, particles with positive or negative impact parameters may exist. $\rho_1(0, 1)$ is the dotted curve plotted in Fig. 6. $\rho_1(-1, 1)$ is the boundary of the completely shielded region. Particles within the volume bounded by these two surfaces have impact parameters within the interval $-1.0 \leq \bar{\gamma} \leq 0$. We notice that the partially shielded region lies within this volume. Consequently, particles existing within the partially shielded region must have impact parameters within the interval $-1.0 \leq \bar{\gamma} \leq 0$. Other curves $\rho_1(\bar{\gamma}_1, 1)$, $-1.0 < \bar{\gamma}_1 \leq 0$ could be plotted

on the (ρ, θ) plane. These curves would fall inside $\rho_1(0, 1)$. Particles with impact parameters within the interval $0 \leq \bar{\gamma} \leq \bar{\gamma}_1$ may exist anywhere inside these surfaces except within the totally shielded region. Thus only particles with a definable range of impact parameters can exist within a small volume within the partially shielded region. This range lies within the interval $-1.0 \leq \bar{\gamma} \leq 0$.

The advantage of the above approach is that we can find easily the range of impact parameters that particles must have to exist within a given arbitrary volume in Störmer space, given an isotropic distribution at infinity. We note that we have studied the behavior of the inner forbidden region $\rho_1(\gamma, 1)$ with varying impact parameter to determine the range of impact parameters particles must have to exist within a given volume in Störmer space. We studied the inner and outer forbidden regions to determine the allowed solid angle at all points in Störmer space, given an isotropic distribution at infinity.

Given a point in Störmer space, we can also determine the range of impact parameters of particles passing through the point. The cone half angle of the allowed solid angle at any point within the partially shielded region is given by Eq. (III-23) and $2\bar{\gamma}$ is given by Eq. (III-27). The range of impact parameters of particles passing through a point (ρ, θ) within the partially shielded region can be found by allowing Q of Eq. (III-27) to take on values from 1 to Q_c . Similarly the range of impact parameters of particles passing through a point (ρ, θ) anywhere within the unshielded region can be found by allowing Q to take on values from 1.0 to -1.0.

Number density $f(\vec{r})$ with units of particles/cm³ is defined in terms of the flux by

$$f(\vec{r}) = \frac{\Phi(\vec{r})}{v} \quad . \quad (\text{III-29})$$

Dividing Eqs. (III-24), (III-25), and (III-26) by v , we obtain the number of density ratio at any point in space:

$$\frac{f(\vec{r})}{f(\vec{r}_\infty)} = 0 \quad \text{if} \quad Q_c \geq 1.0 \quad (\text{III-30})$$

$$\frac{f(\vec{r})}{f(\vec{r}_\infty)} = 1.0 \begin{cases} \text{if } Q_c \leq -1.0 \\ \text{if } -1.0 < Q_c < 0 \text{ and } \frac{\partial Q_c}{\partial \rho} > 0 \end{cases} \quad (\text{III-31})$$

$$\frac{f(\vec{r})}{f(\vec{r}_\infty)} = \frac{1}{2} [1 - Q_c] \text{ if } -1.0 < Q_c < 1.0 \text{ and } \frac{\partial Q_c}{\partial \rho} < 0 \quad (\text{III-32})$$

D. Isotropic, Continuous Energy Distribution Homogeneously Distributed an Infinite Distance Away From the Infinitesimal Dipole

1. Integrated Differential Number Spectrum or Flux Spectrum

In this section, we shall determine the flux spectrum and cutoff momentum or energy at any point in real space. We shall study the mapping of a given point (r, θ, ϕ) in real space into Störmer space (ρ, θ, ϕ) under the Störmer transformation, with particle energy as the variable.

A continuous flux distribution in energy can be thought of as made up of many monoenergetic distributions of varying intensity. Given the energy spectrum of the flux at \vec{r}_∞ , the energy spectrum at \vec{r} can be computed at as many energy points as desired using the derived Eqs. (III-24), (III-25), and (III-26) for the monoenergetic distribution. Rewriting these equations to emphasize their energy dependence:

$$\frac{\Phi(\vec{r})}{\Phi(\vec{r}_\infty)} = 0 \text{ if } Q_c(T) \geq 1.0$$

$$\frac{\Phi(\vec{r})}{\Phi(\vec{r}_\infty)} = 1 \begin{cases} \text{if } Q_c(T) \leq -1.0 \\ \text{if } -1.0 < Q_c(T) < 0 \text{ and } \frac{\partial Q_c}{\partial \rho} > 0 \end{cases}$$

$$\frac{\Phi(\vec{r})}{\Phi(\vec{r}_\infty)} = \frac{1}{2} [1 - Q_c(T)] \text{ if } -1.0 < Q_c(T) < 1.0 \text{ and } \frac{\partial Q_c}{\partial \rho} < 0$$

$$Q_c(T) = \frac{C_{st}^2(T) \sin \theta}{r^2} - \frac{2 C_{st}(T)}{r \sin \theta}$$

However, we must determine the cutoff energy at point (r, θ, ϕ) . Considering the Störmer transformation $\rho = r/C_{st}(T)$, point (r, θ, ϕ) maps multiply into Störmer space (ρ, θ, ϕ) as the particle energy varies (see Fig. 7). Particle energies corresponding to points falling within the totally shielded region will not be seen at point (r, θ, ϕ) . Particle energies corresponding to points falling within the partially shielded region will be seen at point (r, θ, ϕ) within an allowed solid angle less than 4π . Particle energies corresponding to points falling within the unshielded region will be seen at point (r, θ, ϕ) over a 4π solid angle. The totally shielded region is distinguished by the fact that $Q_c(T) \geq 1$. Outside this region $Q_c(T) < 1$. Solving Eqs.(II-14) and (II-11) for the momentum:

$$p = \frac{qM\rho^2}{4\pi r^2} . \quad (\text{III-33})$$

We note that the particle momentum is proportional to ρ^2 , if the particle is allowed at (ρ, θ) . Consequently, the maximum particle momentum not seen at (r, θ, ϕ) corresponds to the point falling on the boundary $\rho_1(\bar{\gamma}_c, 1)$ of the totally shielded region.

Given the arbitrary continuous spectra and notation of Fig. 8 and a point (r, θ, ϕ) then:

$$p_{\text{cutoff}}(\bar{\gamma}_c, 1) = \frac{qM\rho^2(\bar{\gamma}_c, 1)}{4\pi r^2} \quad \text{if } Q_c(p_{\text{min}}) \geq 1.0 \quad (\text{III-34})$$

$$p_{\text{cutoff}}(\bar{\gamma}_c, 1) = p_{\text{min}} \quad \text{if } Q_c(p_{\text{min}}) < 1.0 . \quad (\text{III-35})$$

Of course, the cutoff energy $T_{\text{cutoff}}(\bar{\gamma}_c, 1)$ is related to the cutoff momentum by the relativistic equation:

$$T(\bar{\gamma}, Q) = [p^2(\bar{\gamma}, Q) c^2 + m^2 c^4]^{\frac{1}{2}} - mc^2 . \quad (\text{III-36})$$

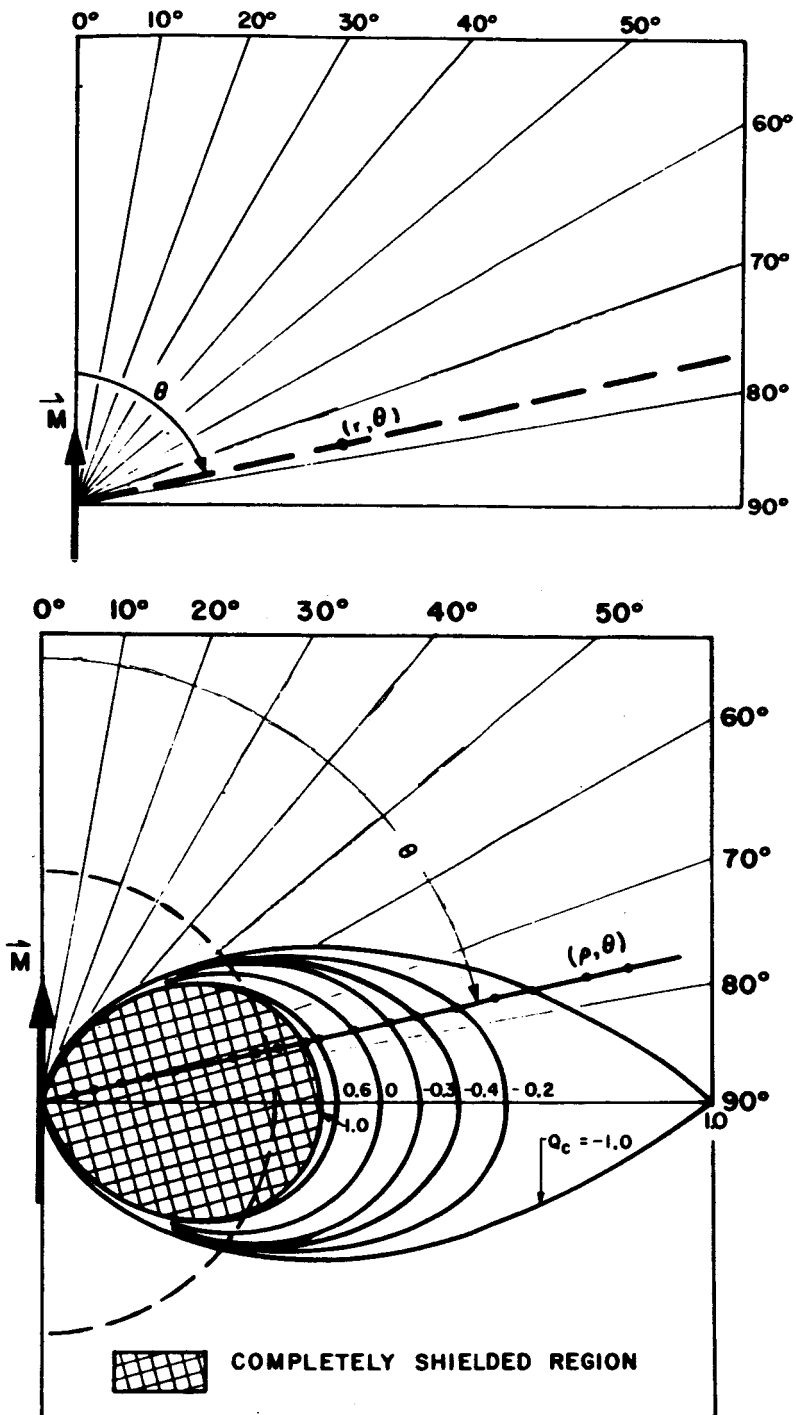


Fig.7-MAPPING OF POINT (r, θ) INTO THE (ρ, θ) PLANE via THE STÖRMER TRANSFORMATION.

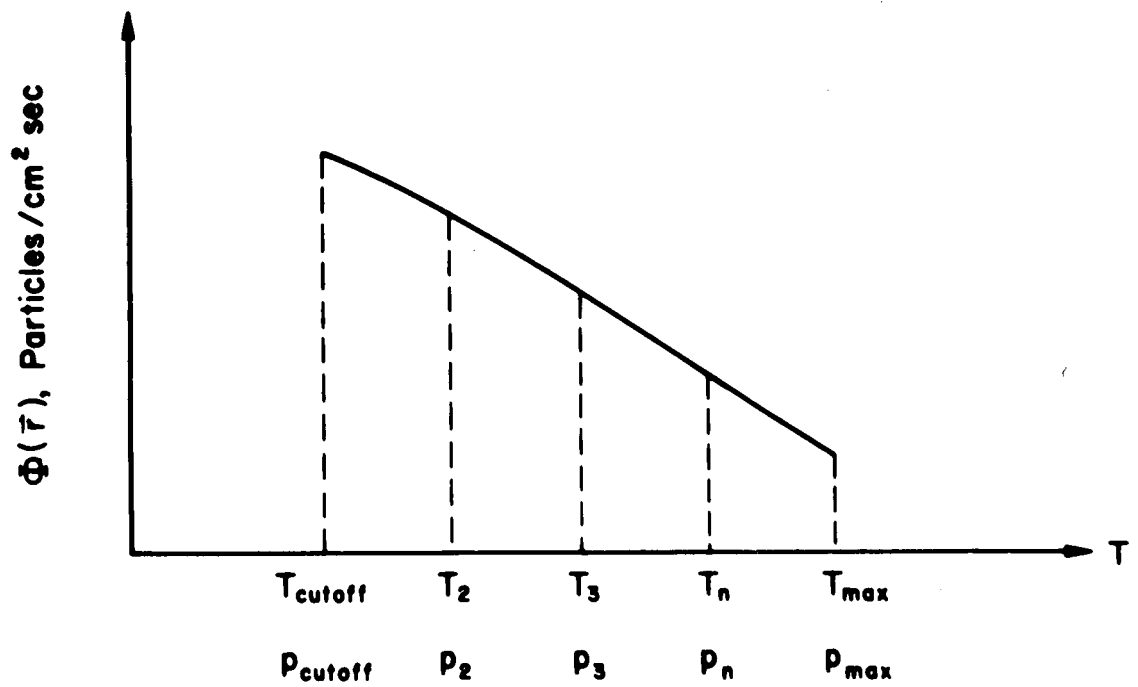
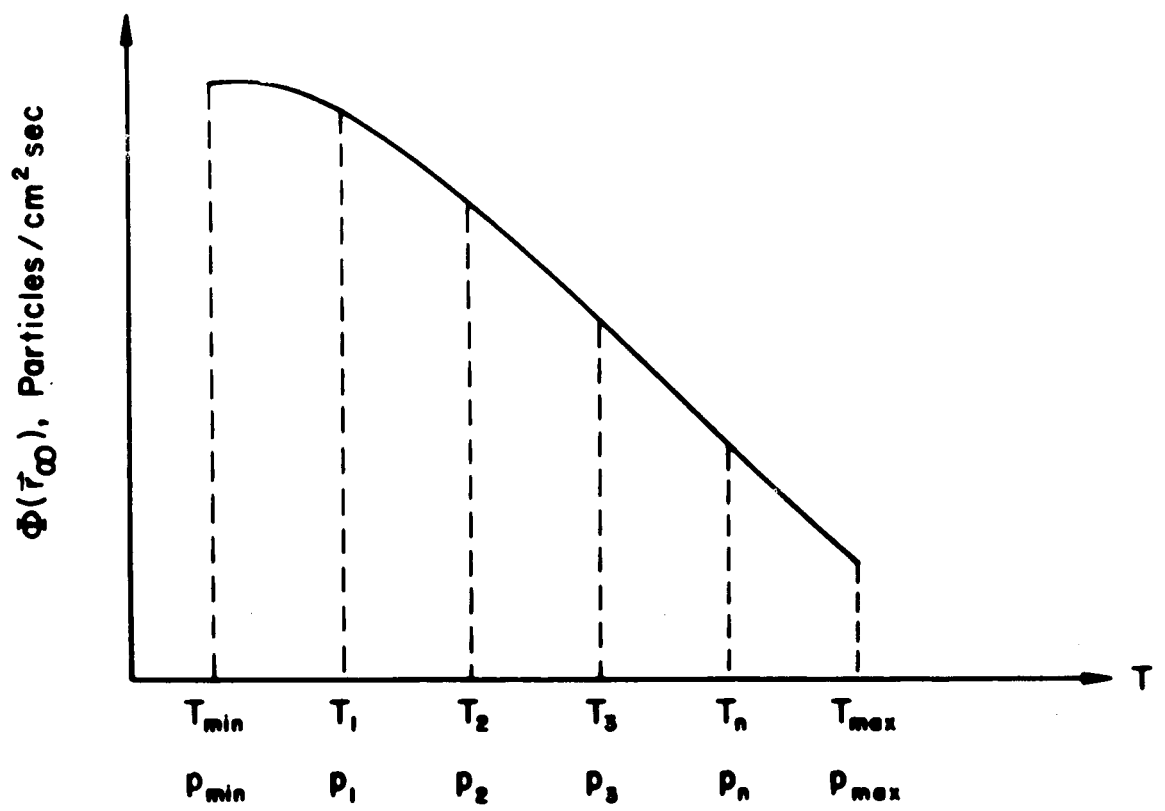


Fig. 8-ARBITRARY FLUX SPECTRUM AT \vec{r} AND \vec{r}_∞ .

Other curves of constant Q_C are also plotted in Fig. 7. We notice that other cutoff momenta can be defined, keeping in mind the mapping of (r, θ, ϕ) into Störmer space as particle energy varies. The maximum particle momentum not seen at (r, θ, ϕ) within a cone with half angle $\cos^{-1} Q_C$ corresponds to the point falling on the boundary $\rho(\bar{\gamma}_C, Q_C)$. Particles with momenta less than $p_{\text{cutoff}}(\bar{\gamma}_C, Q_C)$ are allowed anywhere within this cone of directions and are forbidden outside. This cone opens up as the particle momentum increases. Figures 9 and 10 show the cutoff energy for protons versus angle $\cos^{-1} Q_C$ above the eastern horizon at various magnetic colatitudes on the surface of a spherical spaceship with a 10 meter radius and a dipole moment of 2.51×10^5 weber-meters. For the earth and for our spaceship $M/r^2 = 2.51 \times 10^7$ webers/meter.

The allowed cone is just closed for particle momentum

$$p_{\text{cutoff}}(-1, 1) = \frac{qM}{4\pi r^2} \left[\frac{\sin^2 \theta}{1 + \sqrt{1 + \sin^3 \theta}} \right]. \quad (\text{III-37})$$

The cone is half open for particle momenta less than

$$p_{\text{cutoff}}(-1, 0) = \frac{qM \sin^4 \theta}{4\pi r^2} \quad (\text{III-38})$$

and greater than $p_{\text{cutoff}}(-1, 1)$. The cone is fully open for particle momenta less than

$$p_{\text{cutoff}}(-1, -1) = \frac{qM}{4\pi r^2} \left[\frac{\sin^2 \theta}{1 + \sqrt{1 - \sin^3 \theta}} \right]^2 \quad (\text{III-39})$$

and greater than $p_{\text{cutoff}}(-1, 1)$.

Let us turn our attention to the flux ratio. The flux ratio at point (r, θ, ϕ) is < 1.0 in the momentum range $p_1(1, 1) < p < p_2(-1, -1)$ and is equal to 1.0 for $p \geq p_2(-1, -1)$ where $p(\bar{\gamma}, Q) \equiv [qM/4\pi r^2] \rho^2(\bar{\gamma}, Q)$. By Eq. (III-33) the particle momentum is proportional to ρ^2 . However, the functional dependence of T upon ρ varies with energy, being proportional to ρ^2 at relativistic energies and to ρ^4 at nonrelativistic

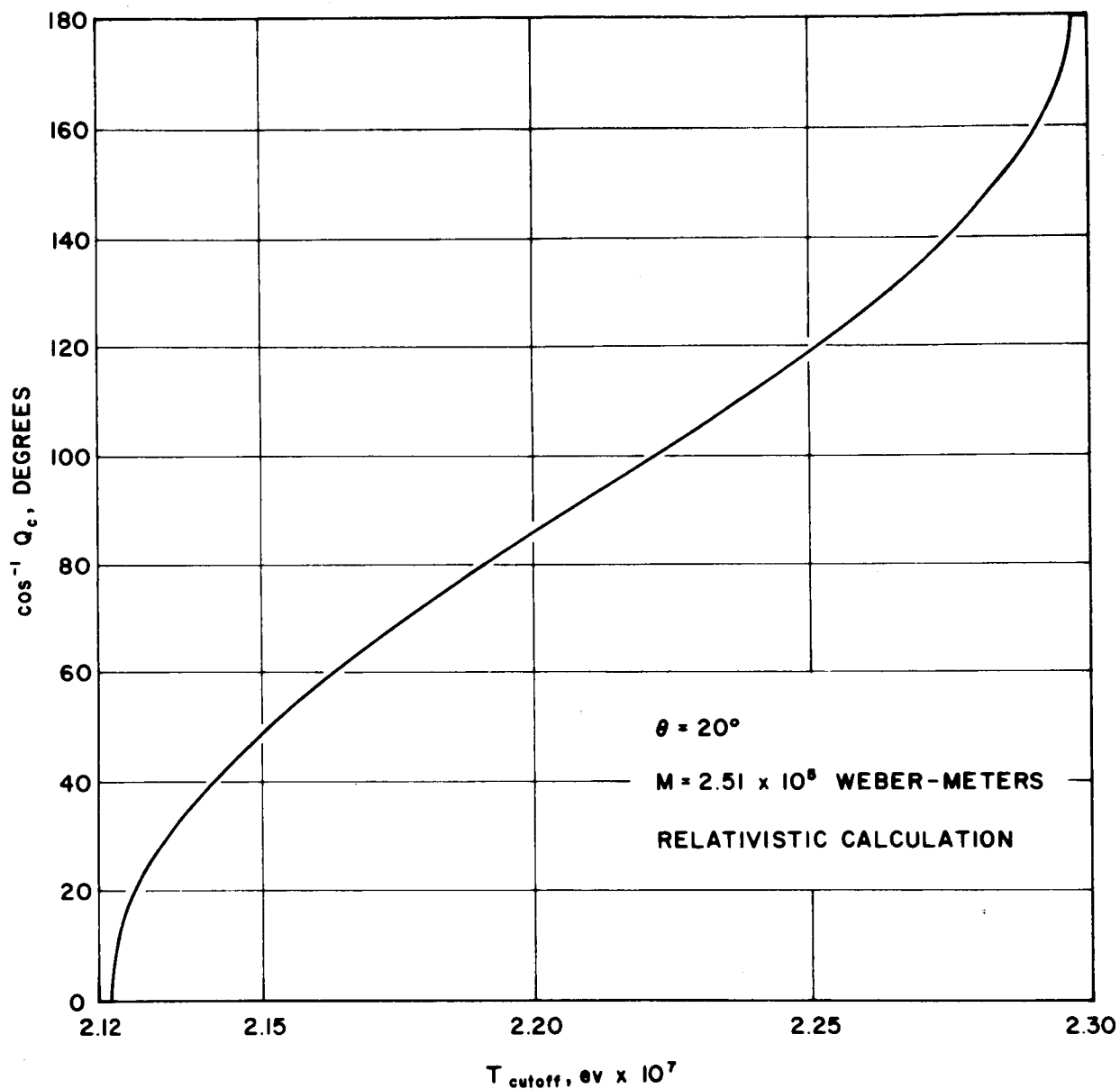


Fig.9-CONE HALF ANGLE ABOVE THE EASTERN HORIZON OF A 20 METER SPHERE FOR PROTONS VERSUS CUTOFF ENERGY. THE INFINITESIMAL DIPOLE IS LOCATED AT THE CENTER OF THE SPHERE.

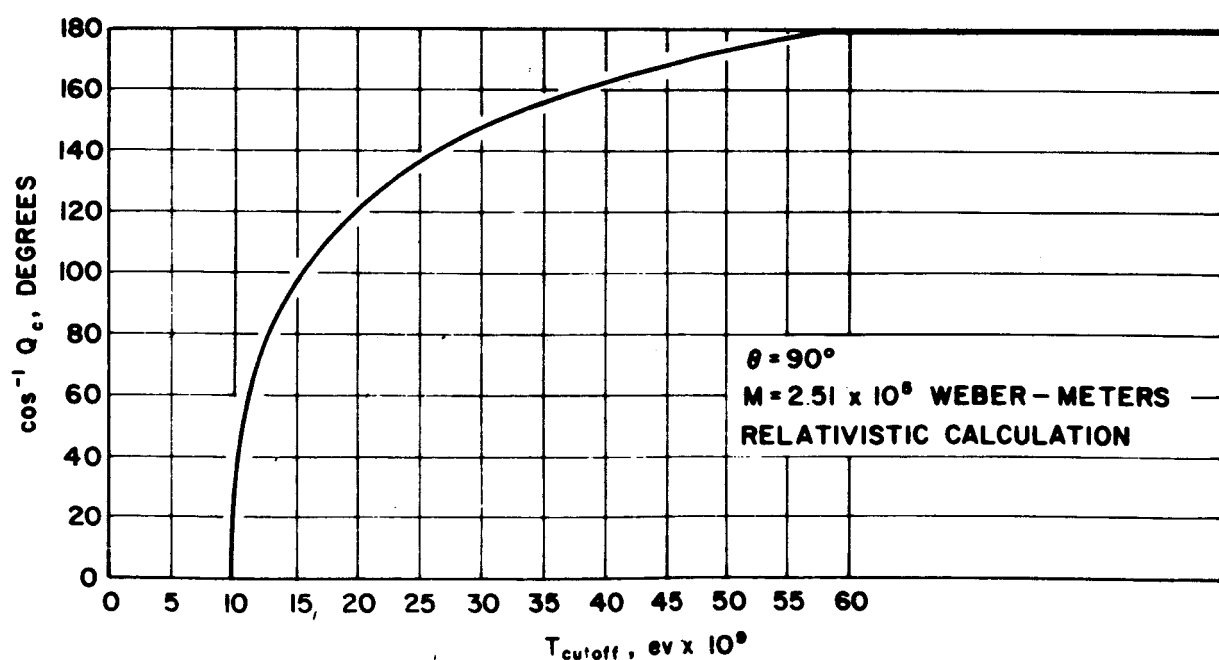
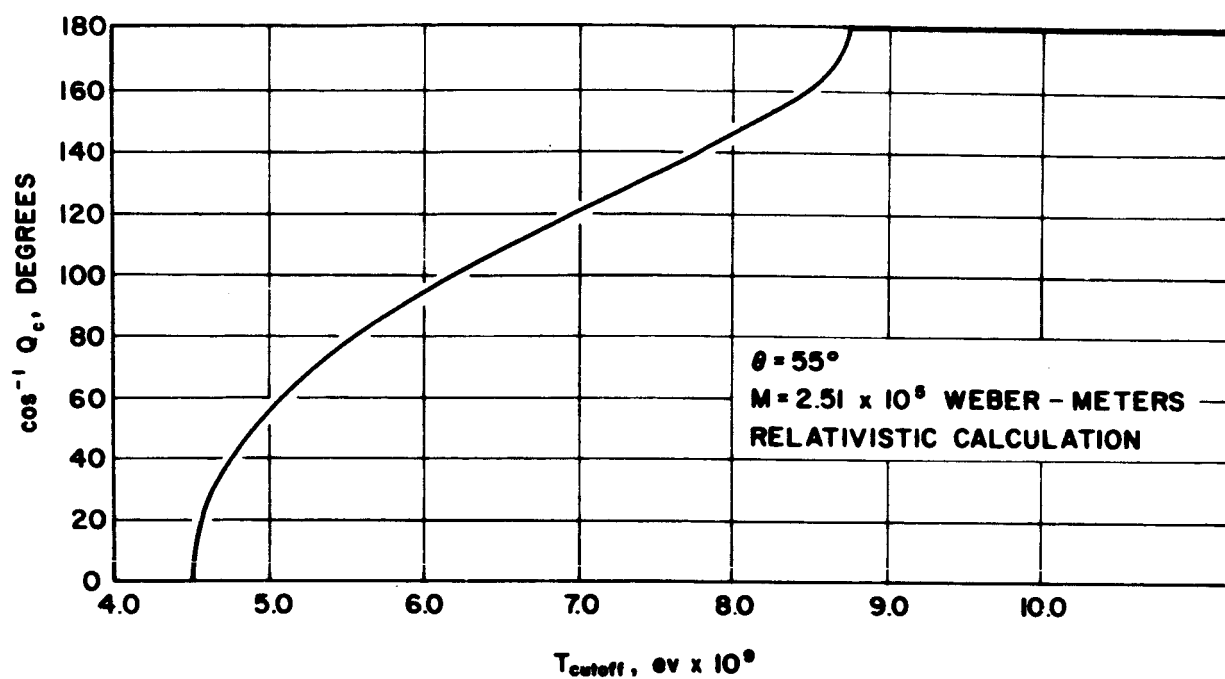


Fig. 10- CONE HALF ANGLE ABOVE THE EASTERN HORIZON OF A 20 METER SPHERE FOR PROTONS VERSUS CUTOFF ENERGY. THE INFINITESIMAL DIPOLE IS LOCATED AT THE CENTER OF THE SPHERE.

energies. Since $\rho_1(-1, 1) \leq \rho_2(-1, -1) \leq 1.0$, the relativistic effect results in a smaller spread of energy where the flux ratio is less than 1.0. The flux ratio at these energies, on our sphere, is proportional to $1 - T^{-1/2}$ at nonrelativistic energies becoming proportional to $1 - T^{-1}$ at relativistic energies in the middle and low latitudes for particles with $C_{st} \gg 1.0$. Because $T_1(-1, 1) \cong T_2(-1, -1)$ in the higher latitudes, the flux ratio is approximately a linear function of energy. Since the difference $T_1(-1, 1) - T_2(-1, -1)$ increases with decreasing latitude and since their magnitudes increase with decreasing latitude, the flux ratio becomes very nearly proportional to $1 - T^{-1}$ in the energy range $T_1(-1, 1) < T < T_2(-1, -1)$ on the equator. Figures 11 and 12 show this type of behavior.

The number density spectrum at point (r, θ, ϕ) can be found in exactly the same manner as the flux spectrum with a cutoff momentum given by Eqs. (III-34) and (III-35).

2. Differential Number Spectrum

Since we know the cutoff momentum and the allowed solid angle as a function of particle energy at point (r, θ, ϕ) , the differential number spectrum is easily found. Differential number spectrum is defined by the integral

$$N(\vec{r}, T) \equiv \int_{\Omega(\vec{r})} v f(\vec{r}, T, \hat{\Omega}) d\Omega \equiv \int_{\Omega(\vec{r})} N(\vec{r}, T, \hat{\Omega}) d\Omega \frac{\text{particles}}{\text{cm}^2 \text{ sec Mev}} \quad (\text{III-40})$$

Let $N(\vec{r}, T, \hat{\Omega})_{\infty} = N(\vec{r}, T, \hat{\Omega}_{iso})_{\infty}$; i. e., an isotropic, homogeneous, continuous energy spectrum at infinity. The differential number spectrum ratio is

$$\frac{N(\vec{r}, T)}{N(\vec{r}_{\infty}, T)} = \frac{\int_{\Omega(\vec{r})} N(\vec{r}, T, \hat{\Omega}) d\Omega}{\int_{\Omega(\vec{r}_{\infty})} N(\vec{r}, T, \hat{\Omega})_{\infty} d\Omega} \quad (\text{III-41})$$

Invoking Liouville's theorem:

$$N(\vec{r}, T, \hat{\Omega}) = N(\vec{r}, T, \hat{\Omega})_{\infty} \equiv N(\vec{r}, T, \hat{\Omega}_{iso})_{\infty}$$

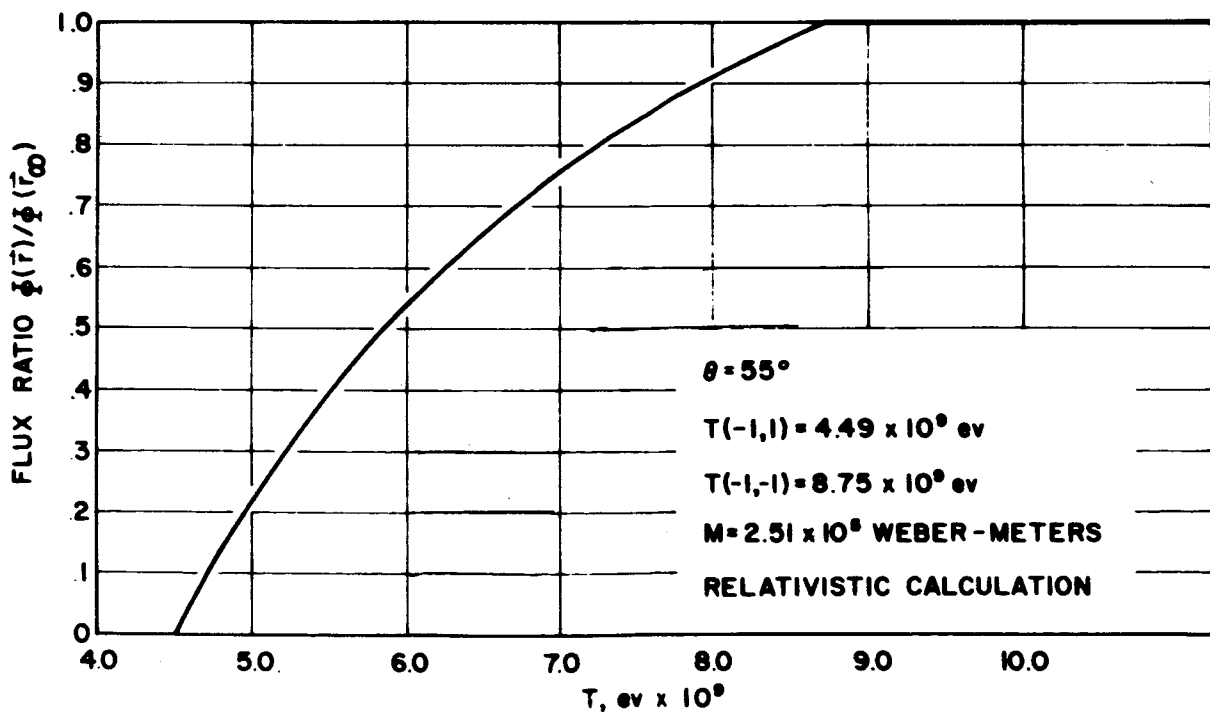
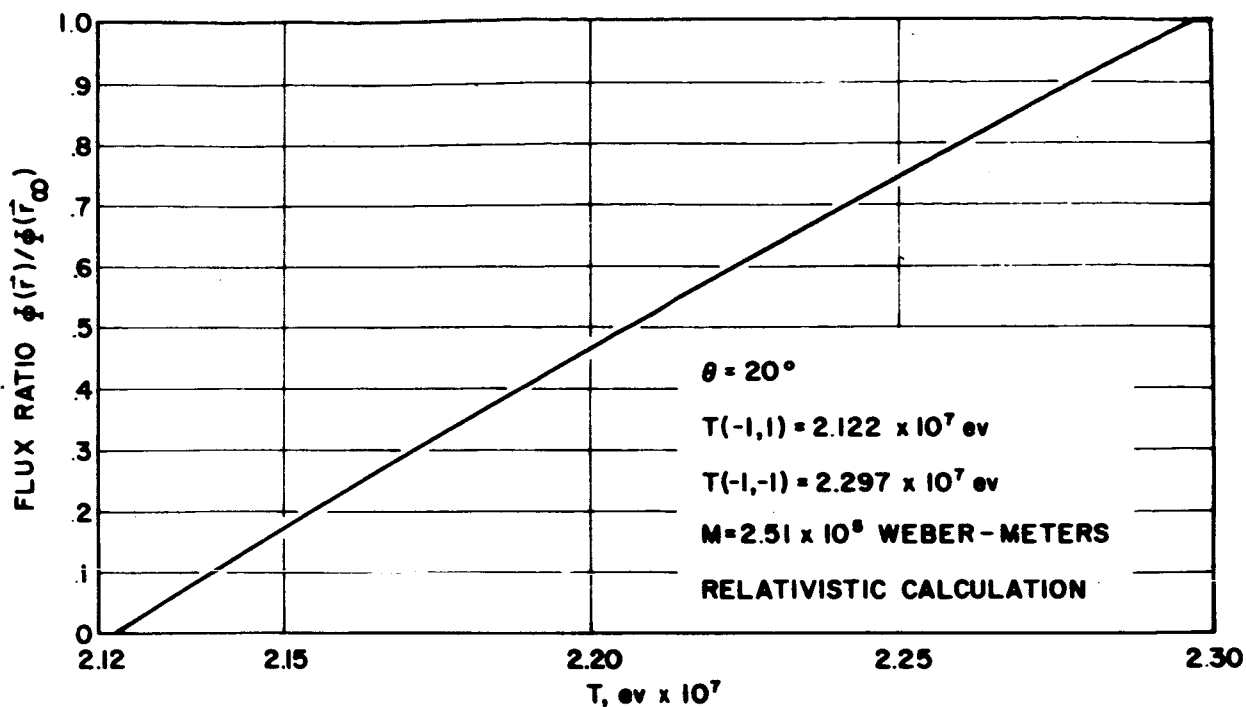


Fig. II-RELATIVISTIC PROTON FLUX RATIO TEN METERS FROM
 A DIPOLE AT SELECT MAGNETIC CO-LATITUDES.

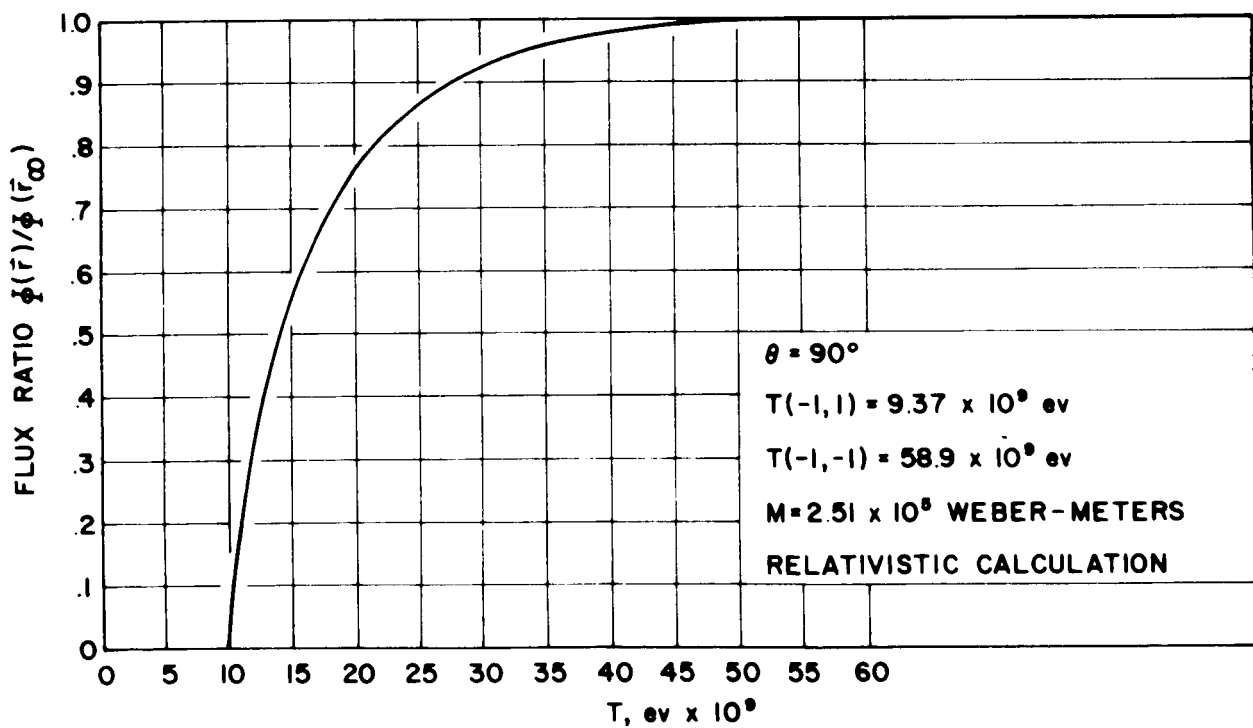
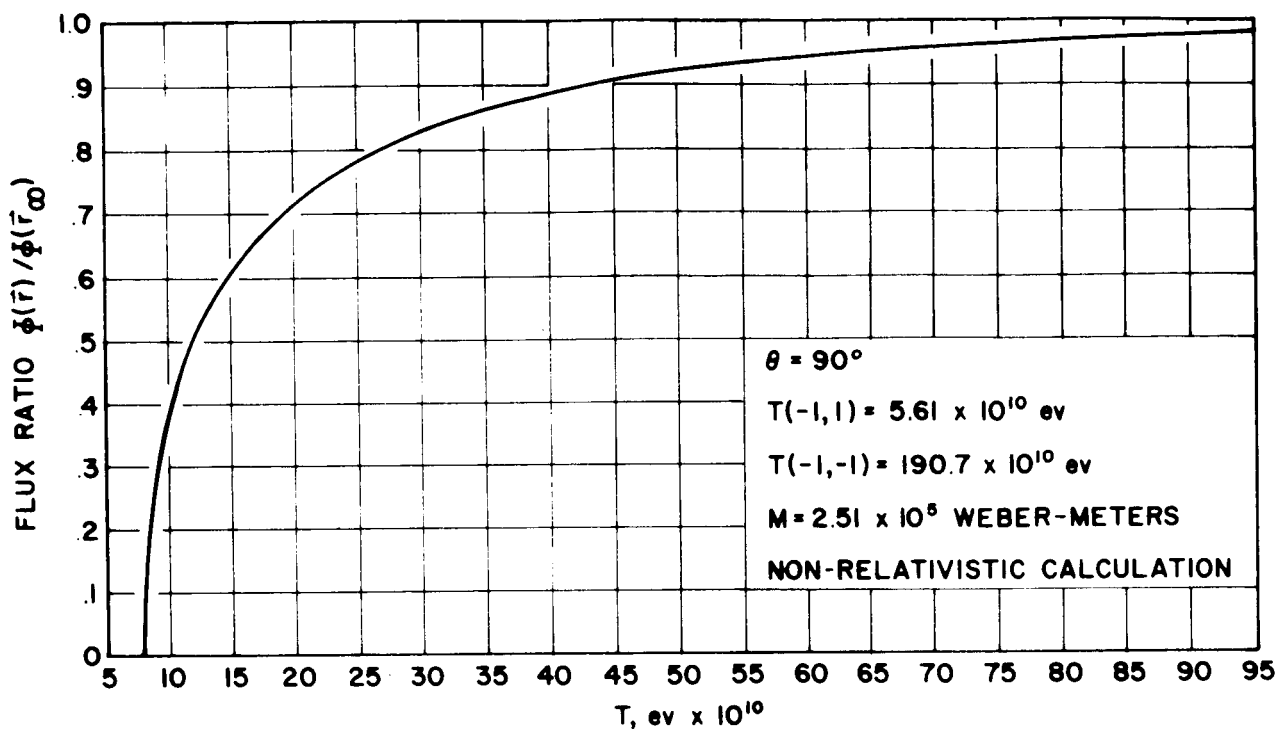


Fig. 12-RELATIVISTIC AND NON-RELATIVISTIC PROTON FLUX RATIO TEN METERS FROM A DIPOLE ON THE MAGNETIC EQUATOR.

Eq. (III-41) becomes

$$\frac{N(\vec{r}, T)}{N(\vec{r}_\infty, T)} = \frac{2\pi[Q_1(T) - Q_2(T)]}{C(T)} \quad (\text{III-42})$$

where

$$C(T) \equiv \int_{\Omega(\vec{r}_\infty)} N(\vec{r}, T, \hat{\Omega}_{iso})_\infty d\Omega. \quad (\text{III-43})$$

The problem of determining the limits in Eq. (III-42) is the same problem previously encountered in the last section. Consequently,

$$\frac{N(\vec{r}, T)}{N(\vec{r}_\infty, T)} = 0 \quad \text{if } Q_c(T) \geq 1.0 \quad (\text{III-44})$$

$$\frac{N(\vec{r}, T)}{N(\vec{r}_\infty, T)} = 1.0 \quad \begin{cases} \text{if } Q_c(T) \leq -1.0 \\ \text{if } -1.0 < Q_c(T) < 0 \text{ and } \frac{\partial Q_c}{\partial \rho} > 0 \end{cases} \quad (\text{III-45})$$

$$\frac{N(\vec{r}, T)}{N(\vec{r}_\infty, T)} = \frac{2\pi[1 - Q_c(T)]}{C(T)} \quad \text{if } -1.0 < Q_c(T) < 1.0 \text{ and } \frac{\partial Q_c}{\partial \rho} < 0. \quad (\text{III-46})$$

Likewise, the cutoff momentum at point (r, θ, ϕ) is given by Eqs. (III-34) and (III-35).

3. Volume Integral of the Particle Density and Shielding Effectiveness of the Partially Shielded Region

A figure of merit or omnidirectional attenuation factor which describes the effectiveness of the magnetic field as a shield against particles impinging upon volume V from all allowed directions is defined:

$$F(\vec{\rho}) = \frac{\text{number of particles within volume } V(\vec{\rho}) \text{ with the magnetic field absent}}{\text{number of particles within volume } V(\vec{\rho}) \text{ with the magnetic field present}} \quad (\text{III-47})$$

$$= \frac{1}{\text{fraction of the number of particles permitted to enter } V(\vec{\rho})}$$

$$F(\vec{\rho}) \equiv \frac{g(\vec{\rho}_\infty)}{g(\vec{\rho})} \quad (\text{III-48})$$

We have mapped our volume into Störmer space via the Störmer transformation. If the volume to be shielded lies wholly within the totally shielded region, $F = \infty$ corresponding to an infinite attenuation coefficient. If any of the volume to be shielded falls outside the totally shielded region $F < \infty$. To shield a crew compartment completely against a monoenergetic, isotropic distribution of protons, the crew compartment should be an oval toroid encompassing the entire totally shielded region. The magnetic moment of the dipole field will be a minimum under these conditions. The number of particles within volume $V(\vec{\rho})$ with the field present is:

$$g(\vec{\rho}) = \int_V f(\vec{\rho}) dV = \int \int \int f(\vec{\rho}) C_{st}^3 \rho^2 \sin \theta d\rho d\theta d\phi. \quad (\text{III-49})$$

The number of particles within volume V with the field absent is equal to the number of particles within volume V at infinity;

$$g(\vec{\rho}_\infty) = \int_V f(\vec{\rho}_\infty) dV = \int \int \int f(\vec{\rho}_\infty) C_{st}^3 \rho^2 \sin \theta d\rho d\theta d\phi. \quad (\text{III-50})$$

Assuming the distribution is monoenergetic at infinity,

$$F(\vec{\rho}) = \frac{\int \int \int f(\vec{\rho}_\infty) \rho^2 \sin \theta d\rho d\theta d\phi}{\int \int \int f(\vec{\rho}) \rho^2 \sin \theta d\rho d\theta d\phi} \quad (\text{III-51})$$

If the distribution is isotropic at infinity, Eqs. (III-29), (III-30), and (III-31) provide $f(\rho)$. Let us compute the attenuation factor of the partially shielded region:

$$F(\vec{\rho}) = \frac{\int_0^{2\pi} \int_0^\pi \int_{\rho_1(-1,1)}^{\rho_2(-1,-1)} f(\vec{\rho}_\infty) \rho^2 \sin \theta \, d\rho \, d\theta \, d\phi}{\int_0^{2\pi} \int_0^\pi \int_{\rho_1(-1,1)}^{\rho_2(-1,-1)} \frac{f(\vec{\rho}_\infty)}{2} \left[1 - \frac{\sin \theta}{\rho^2} + \frac{2}{\rho \sin \theta} \right] \rho^2 \sin \theta \, d\rho \, d\theta \, d\phi} \quad (\text{III-52})$$

$$F(\vec{\rho}) = \frac{2}{1 - \frac{\int_0^\pi \int_{\rho_1}^{\rho_2} [\sin^2 \theta - 2\rho] \, d\rho \, d\theta}{\int_0^\pi \int_{\rho_1}^{\rho_2} \rho^2 \sin \theta \, d\rho \, d\theta}} \quad (\text{III-53})$$

where

$$\left. \begin{aligned} \rho_1(-1, 1) &= \frac{\sin^2 \theta}{1 + \sqrt{1 + \sin^3 \theta}} \\ \rho_2(-1, -1) &= \frac{\sin^2 \theta}{1 + \sqrt{1 - \sin^3 \theta}} \end{aligned} \right\} \quad (\text{III-54})$$

Equation (III-53) was integrated over ρ first and then numerically integrated over θ using Simpson's rule with $\Delta\theta = 0.5^\circ$ giving the result $\rightarrow F(\vec{\rho}) = 1.22$. To interpret this number, let us map the totally and partially shielded regions into real space and disregard any specific volume to be shielded. The partially shielded region is simply a semi-transparent region adjacent to the opaque totally shielded region whose omnidirectional attenuation coefficient is 1.22, independent of the impinging particles' momentum, charge, or dipole moment of the field. The physical dimensions of these regions are, importantly, functions of these three parameters, i.e., the particle Störmer radius.

Let us compute the volume of the totally and partially shielded regions, i.e.,

$$V \left| \begin{array}{l} \rho_1(-1, 1) \\ 0 \end{array} \right. = 2\pi C_{st}^3 \int_0^\pi \int_0^{\rho_1(-1, 1)} \rho^2 \sin \theta \, d\rho d\theta = 0.147 C_{st}^3 \quad (\text{III-55})$$

$$V \left| \begin{array}{l} \rho_2(-1, -1) \\ \rho_1(-1, 1) \end{array} \right. = 2\pi C_{st}^3 \int_0^\pi \int_{\rho_1(-1, 1)}^{\rho_2(-1, -1)} \rho^2 \sin \theta \, d\rho d\theta = 0.808 C_{st}^3 \quad (\text{III-56})$$

The above integrals were evaluated numerically using Simpson's rule with $\Delta\theta = 0.5^\circ$. The partially shielded region is approximately 5.5 times the volume of the totally shielded region. Of course, these volumes are a function of the particle Störmer radius and can be very large for low energy particles as we shall observe in a later section.

Let us consider two specific volumes to be shielded to examine the directional shielding provided by the dipole field over the surfaces of these volumes for monoenergetic particles. Let the first volume be a sphere (dotted curve in Fig. 7) with the dipole at its center. The low latitudes near the equator are completely shielded, the middle latitudes are partially shielded and the high latitudes are completely unshielded. For a given small distance inside the surface of the sphere, the allowed solid angles in the high latitudes are greater than the allowed solid angles on the equator. Consider an oval-shaped toroid whose surface coincides with the outer surface of the partially shielded region. The high latitudes are shielded better than the low latitudes. For a given small distance inside the surface of the toroid, the allowed solid angles in the low latitudes are greater than the allowed solid angles in the high latitudes — diametrically opposite to the spherical case. The determination of the optimum shaped volume for a given particle energy distribution is a subject we shall not investigate in this paper.

4. Constant Flux Surfaces

In this section we will study the constant flux contour surfaces to gain a better understanding of the allowed solid angle and momentum cutout at any point in a particular magnetic field. Let f be the flux

ratio. From Eq. (III-31), in the partially shielded region,

$$\frac{\Phi(\vec{r})}{\Phi(\vec{r}_\infty)} \equiv f = \frac{1}{2} \left[1 - \frac{C_{st}^2 \sin \theta}{r^2} + \frac{2C_{st}}{r \sin \theta} \right]. \quad (\text{III-57})$$

Rewriting Eq. (III-57) in cylindrical coordinates (R, ϕ, z) ,

$$2f = 1 - \frac{C_{st}^2 R}{[R^2 + z^2]^{3/2}} + \frac{2C_{st}}{R}. \quad (\text{III-58})$$

To determine the curves of constant flux in the equatorial plane we set $z = 0$ and solve for R ,

$$[2f - 1] R^2 - 2R C_{st} + C_{st}^2 = 0 \quad (\text{III-59})$$

$$R = C_{st} \left[\frac{1 \pm \sqrt{2[1 - f]}}{2f - 1} \right]; \quad f \neq \frac{1}{2} \quad (\text{III-60})$$

$$R = \frac{C_{st}}{2}; \quad f = \frac{1}{2} \quad (\text{III-61})$$

To determine which sign must be chosen in Eq. (III-60), we will let f be greater than and less than $1/2$. If $f < 1/2$, Eq. (III-60) becomes

$$R = C_{st} \left[\frac{1 \pm \sqrt{2[1 - f]}}{-|2f - 1|} \right]. \quad (\text{III-62})$$

We choose the minus sign so that R will be positive. If $f > 1/2$, Eq. (III-60) becomes

$$R = C_{st} \left[\frac{1 \pm \sqrt{2[1 - f]}}{|2f - 1|} \right]. \quad (\text{III-63})$$

If we choose the positive sign, R can be greater than C_{st} and double valued. But we know that the Störmer transformation is a linear transformation and that the constant f surfaces lie in the partially shielded region:

$$C_{st}[\sqrt{2} - 1] \leq R \leq 1.0 C_{st} \text{ for } 0 \leq f \leq 1.0 .$$

Therefore, we choose the negative sign again and

$$R = C_{st} \left[\frac{1 - \sqrt{2[1 - f]}}{2f - 1} \right] ; f \neq \frac{1}{2} . \quad (\text{III-64})$$

Substituting for C_{st} and solving for the particle momentum,

$$p^{\frac{1}{2}} = \left[\frac{qM}{4\pi R^2} \right]^{\frac{1}{2}} \left[\frac{1 - \sqrt{2[1 - f]}}{2f - 1} \right] ; f \neq \frac{1}{2} . \quad (\text{III-65})$$

$$p^{\frac{1}{2}} = \frac{1}{2} \left[\frac{qM}{4\pi R^2} \right]^{\frac{1}{2}} ; f = \frac{1}{2} . \quad (\text{III-66})$$

Equations (III-65) and (III-66) are plotted in Fig. 13 for singly charged particles in the earth's field. These constant f curves connect points in the equatorial plane which subtend the same allowed solid angle, and therefore are also curves over which the differential number spectrum ratio is equal to f . The constant f curves do not intersect showing that the allowed solid angle is unique at every point in the field for an isotropic, monoenergetic distribution at infinity. The region beneath the $f = 0$ curve is void of particles. The region above the $f = 1.0$ curve subtends a 4π solid angle to the particles.

The curves of constant f in the (R, z) plane, i.e., the meridian plane, are the Störmer curves of constant Q within the inner allowed region for $\bar{\gamma} = -1.0$, and are shown in Fig. 14. The radial coordinate in Störmer units has been converted to earth radii for select proton kinetic energies. The curves are symmetric about the dipole axis

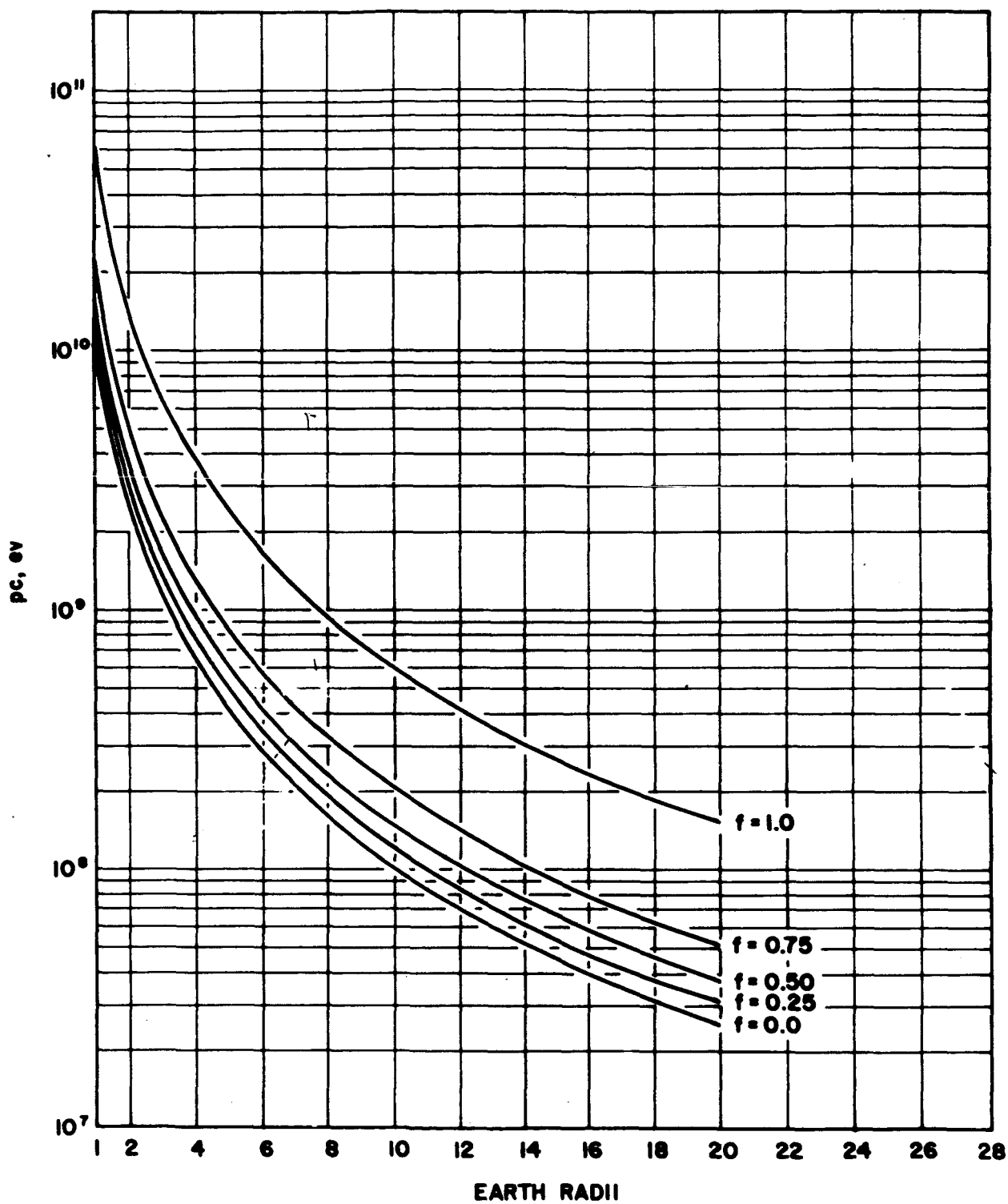


Fig. 13-CONSTANT FLUX RATIO CURVES IN THE EQUATORIAL PLANE OF THE EARTH VERSUS PROTON KINETIC ENERGY.

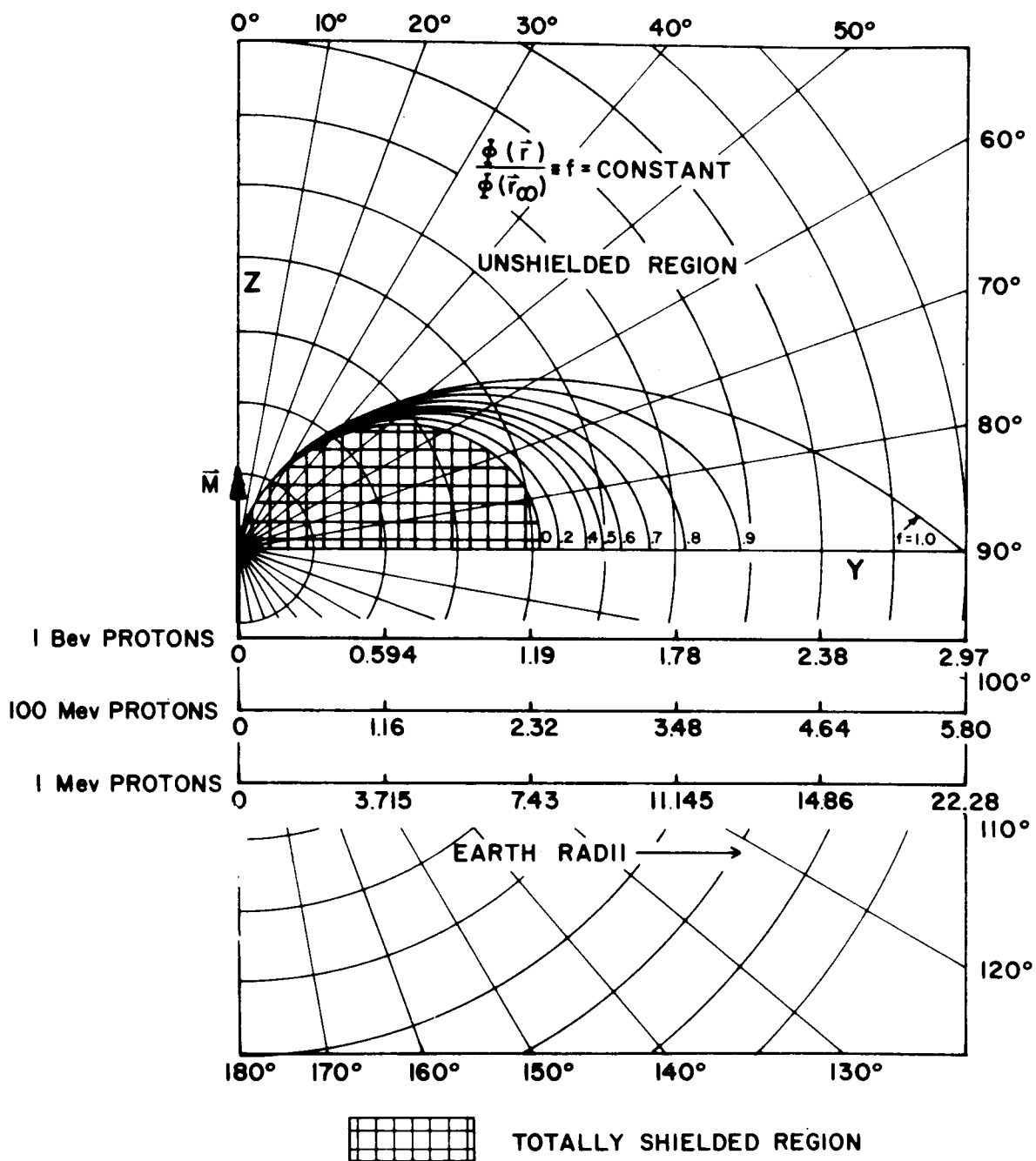


Fig.14-CONSTANT FLUX CONTOURS FOR UNBOUNDED 1 Bev, 100 Mev AND 1 Mev PROTONS IN THE FIELD OF AN INFINITESIMAL MAGNETIC DIPOLE.

and in the x-y plane generating toroidal surfaces in real space. We notice that the constant f surfaces are not uniformly spaced. The surfaces are spread out in the low latitudes encompassing a large region of real space, becoming closer together in the high latitudes. They are infinitesimally close together at the origin. We also observe that the partially shielded region extends out many earth radii in the equatorial plane, beyond the geomagnetic cavity boundary for low energy particles.

IV. PARTICLE DISTRIBUTION IN THE MAGNETIC FIELD OF A FINITE CURRENT LOOP

A. Isotropic, Continuous Energy Distribution Homogeneously Distributed an Infinite Distance Away From the Current Loop

A finite circular current loop of radius, a , consists of a conductor with an infinitesimal cross-sectional area carrying a very large current. As the loop radius approaches zero, the vector potential of the finite dipole approaches the vector potential of the infinitesimal dipole. The vector potential is in the same direction as the current, and the magnetic field is an axially symmetric field about the current loop axis. The loop is in the xy plane with its dipole moment vector directed along the positive z -axis. The vector potential is given by Ref. [8].

$$\vec{A} = \frac{\mu_0 I}{4\pi} \oint \frac{d\vec{r}}{r} \quad (\text{IV-1})$$

$$A_\phi = \frac{Mk^2 C(k)}{\pi^2 a [r^2 + a^2 + 2ar \sin \theta]^{\frac{1}{2}}} \quad (\text{IV-2})$$

where

$$k^2 = \frac{4a r \sin \theta}{r^2 + a^2 + 2ar \sin \theta} \quad (\text{IV-3})$$

$$M \equiv \mu_0 I \pi a^2 \quad .$$

$C(k)$ is a special complete elliptic integral and is defined in terms of the complete elliptic integrals of the first and second kinds [9] :

$$C(k) = \frac{[2 - k^2] K(k) - 2E(k)}{k^4} \quad (\text{IV-4})$$

$$K(k) \equiv \int_0^{\pi/2} \frac{d\phi}{[1 - k^2 \sin^2 \phi]^{1/2}} .$$

$$E(k) \equiv \int_0^{\pi/2} [1 - k^2 \sin^2 \phi]^{1/2} d\phi$$

As $k \rightarrow 0$, $C(k) \rightarrow \pi/16$; and as $k \rightarrow 1$, $C(k) \rightarrow \infty$. The vector potential approaches infinity at the loop and we would expect a forbidden region to exist around the loop. Substituting Eq. (IV-2) in Eq. (II-9):

$$Q = \frac{qMk^2 C(k)}{p\pi^2 a [r^2 + a^2 + 2ar \sin \theta]^{1/2}} + \frac{2\gamma}{r \sin \theta} \quad (\text{IV-5})$$

Dividing the numerator and denominator of the quantities on the right hand side of Eq. (IV-5) by C_{st}^2 and C_{st} respectively:

$$Q = \frac{4k^2 C(k)}{\pi\lambda [\rho^2 + \lambda^2 + 2\lambda\rho \sin \theta]^{1/2}} + \frac{2\bar{\gamma}}{\rho \sin \theta} \quad (\text{IV-6})$$

where

$$\lambda \equiv \frac{a}{C_{st}} \quad (\text{IV-7})$$

$$k^2 = \frac{4\lambda\rho \sin \theta}{\rho^2 + \lambda^2 + 2\lambda\rho \sin \theta} \quad (\text{IV-8})$$

Observe that we have a new parameter λ which is a measure of the particle Störmer radius in comparison to the radius of the loop. Thus, in Störmer space, the boundaries of the forbidden and allowed regions are no longer independent of the particle Störmer radius. Consequently, λ is treated as a new parameter and for a given Q , $\bar{\gamma}$, and λ , Eq. (IV-6) is solved by iteration to find ρ as a function of θ . For a given λ , the forbidden and allowed regions behave exactly in the same manner with varying impact parameter as the forbidden and allowed regions of the infinitesimal dipole. For some large negative $\bar{\gamma}$, the outer forbidden region completely surrounds the inner forbidden

and inner allowed region. At $\bar{\gamma} = 0$, the outer forbidden region disappears. As $\bar{\gamma}$ becomes more positive, the inner forbidden region continues to expand indefinitely. Reference [10] contains a clear description of this behavior. The forbidden and allowed regions have the same properties as the forbidden and allowed regions of the infinitesimal dipole at $\bar{\gamma} = \bar{\gamma}_c$:

$$\text{Inner forbidden region: } Q_c \geq 1.0 \quad (\text{IV-9})$$

$$\text{Outer forbidden region: } Q_c \leq -1.0 \quad (\text{IV-10})$$

$$\text{Inner allowed region: } -1.0 < Q_c < 1.0 \text{ and } \frac{\partial Q_c}{\partial \rho} < 0 \quad (\text{IV-11})$$

$$\text{Outer allowed region: } -1.0 < Q_c < 0 \text{ and } \frac{\partial Q_c}{\partial \rho} > 0$$

The $(\tilde{\rho}, \tilde{\theta})$ coordinate system is defined subsequently. Figure 15 shows the forbidden and allowed regions for three select impact parameters.

Whereas, the outer forbidden region of the infinitesimal dipole pinched off at $\bar{\gamma} = \bar{\gamma}_c = -1.0$, $\bar{\gamma}_c$ is a function of λ for the current loop. A saddle point exists at $\bar{\gamma} = \bar{\gamma}_c$ and the saddle point method treated in Ref. [10] provides the functional dependence of $\bar{\gamma}_c$ upon λ :

$$\left[\frac{\rho_c}{\lambda} \right]^2 - \left[\frac{4B(k)}{\pi\lambda^2} + 1 \right] = 0 \quad (\text{IV-12})$$

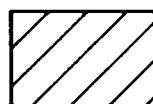
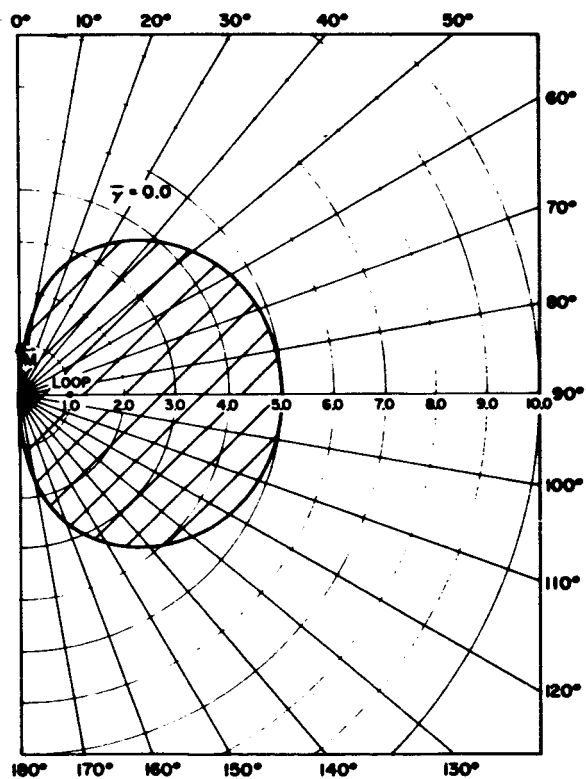
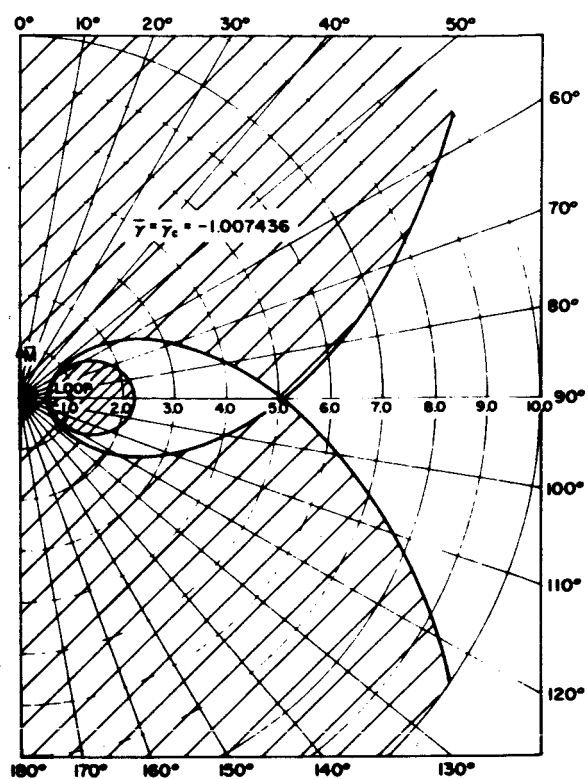
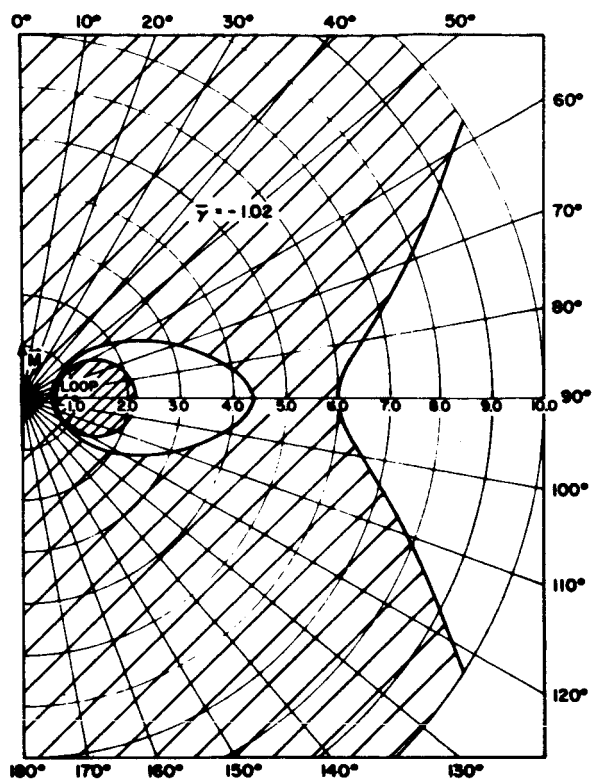
$$\bar{\gamma}_c = \frac{-2\rho_c}{\pi [\rho_c^2 - \lambda^2]} E(k) \quad (\text{IV-13})$$

where

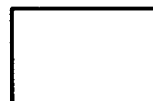
$$k = \frac{\lambda}{\rho_c} \quad (\text{IV-14})$$

$$B(k) = \frac{E(k) + [k^2 - 1] K(k)}{k^2} \quad (\text{IV-15})$$

ρ_c is the radial distance of the saddle point from the origin, in the equatorial plane, of the (ρ, θ) coordinate system.



FORBIDDEN REGION



ALLOWED REGION

Fig.15-ALLOWED AND FORBIDDEN REGIONS OF PARTICLE MOTION IN THE (ρ', θ) PLANE FOR THREE SELECT VALUES OF $\bar{\gamma}$ WITH $\lambda = 0.02$.

Table I gives computed values of $\bar{\gamma}_c$ and ρ_c for select values of λ . Equation (IV-12) is solved by iteration for ρ_c , and $\bar{\gamma}_c$ is then computed from Eq. (IV-13). As $\lambda \rightarrow 0$, $-\bar{\gamma}_c \rightarrow \rho_c \rightarrow 1.0$; and as $\lambda \rightarrow \infty$, $-\bar{\gamma}_c \rightarrow \rho_c/2 \rightarrow \lambda$.

We shift our coordinate system origin to the loop by the transformation:

$$\begin{aligned}\rho \sin \theta &= \lambda + \tilde{\rho} \sin \tilde{\theta} \\ \rho \cos \theta &= \tilde{\rho} \cos \tilde{\theta}\end{aligned}\tag{IV-16}$$

where $(\tilde{\rho}, \tilde{\theta})$ is the polar coordinate system centered on the loop. $\tilde{\theta}$ is measured from the perpendicular to the plane of the loop and $\tilde{\rho}$ is the radial coordinate measured from the loop. Equation (IV-6) becomes:

$$Q = \frac{4k^2 C(k)}{\pi\lambda[\tilde{\rho}^2 + 4\lambda^2 + 4\lambda\tilde{\rho}\sin\tilde{\theta}]^{1/2}} + \frac{2\bar{\gamma}}{\lambda + \tilde{\rho}\sin\tilde{\theta}}\tag{IV-17}$$

where

$$k^2 = \frac{4\lambda[\lambda + \tilde{\rho}\sin\tilde{\theta}]}{\tilde{\rho}^2 + 4\lambda^2 + 4\lambda\tilde{\rho}\sin\tilde{\theta}}.\tag{IV-18}$$

This coordinate system has the advantage that for a given $Q, \lambda, \bar{\gamma}$, and $\tilde{\theta}$; $\tilde{\rho}$ is single valued. We also define a corresponding coordinate system $(\tilde{r}, \tilde{\theta})$ in real space. Rewriting Eq. (IV-17) and setting $\gamma = \gamma_c$:

$$Q_c = \frac{2k^3 C(k)}{\pi\lambda^{3/2}[\lambda + \tilde{\rho}\sin\tilde{\theta}]^{1/2}} + \frac{2\bar{\gamma}_c}{\lambda + \tilde{\rho}\sin\tilde{\theta}}\tag{IV-19}$$

Differentiating Eq. (IV-19) with respect to $\tilde{\rho}$ and employing the necessary differentiation formulae for elliptic integrals in Jahnke and Emde:

TABLE I

Computed Values of $\bar{\gamma}_c$ and ρ_c forSelected Values of λ

λ	$\bar{\gamma}_c$	ρ_c	$\rho'_c \equiv \rho_c/\lambda$
5×10^{-3}	-1.0000044	1.0000438	200.0028767
10^{-2}	-1.0000185	1.0000564	100.0056444
2×10^{-2}	-1.0000749	1.0002250	50.0112522
5×10^{-2}	-1.0004684	1.0014050	20.0281010
10^{-1}	-1.0018709	1.0056047	10.0560472
2×10^{-1}	-1.0074358	1.0221818	5.1109088
3.6×10^{-1}	-1.0236563	1.0697641	2.9715670
5×10^{-1}	-1.0446118	1.1298177	2.2596354
1.0	-1.1598476	1.4405107	1.4405107
2.0	-1.5006854	2.2691984	1.1345992
5.0	-2.8061874	5.1213780	1.0242756
10^1	-5.1959389	10.0626318	1.0062632
2×10^1	-10.1198181	20.0316664	1.0015833
5×10^1	-25.0595632	50.0127189	1.0002544
10^2	-50.0341544	100.0063642	1.0000636
2×10^2	-100.0192378	200.0031828	1.0000159
5×10^2	-250.0068096	500.0012732	1.0000025
10^3	-500.0047909	1000.0006366	1.0000006

$$\frac{\partial Q_c}{\partial \tilde{\rho}} = \frac{-2\bar{\gamma}_c \sin \tilde{\theta}}{[\lambda + \tilde{\rho} \sin \tilde{\theta}]^2} + \frac{-k^3}{\pi \lambda^{3/2} [\lambda + \tilde{\rho} \sin \tilde{\theta}]^{3/2}} \left\{ C(k) \sin \tilde{\theta} + \left[\frac{k^2 \tilde{\rho}}{2\lambda} - [1 - k^2] \sin \tilde{\theta} \right] \left[\frac{D(k) - C(k)}{1 - k^2} \right] \right\} \quad (\text{IV-20})$$

where $D(k)$ is another special complete elliptic integral.

We are now in a position to compute the allowed solid angle at any point in the field. Given a point $(\tilde{r}, \tilde{\theta}, \phi)$ in real space and a loop radius, a , we map the point into $(\tilde{\rho}, \tilde{\theta}, \phi)$ coordinates by the Störmer transformation and Eq. (IV-7). We compute $\bar{\gamma}_c$ from Eqs. (IV-12) and (IV-13). Next we compute Q_c and $\partial Q_c / \partial \tilde{\rho}$ from Eqs. (IV-19) and (IV-20) to determine which of the four regions contains the point. The allowed solid angle Ω is, as in the case of the infinitesimal dipole:

$$\Omega = 0 \quad \text{if} \quad Q_c \geq 1.0 \quad (\text{IV-21})$$

$$\Omega = 4\pi \begin{cases} \text{if } Q_c \leq -1.0 \\ \text{if } -1.0 < Q_c < 0 \text{ and } \frac{\partial Q_c}{\partial \tilde{\rho}} > 0 \end{cases} \quad (\text{IV-22})$$

$$\Omega = 2\pi [1 - Q_c] \quad \text{if} \quad -1.0 < Q_c < 1.0 \text{ and } \frac{\partial Q_c}{\partial \tilde{\rho}} < 0 \quad (\text{IV-23})$$

The momentum cutoff at point $(\tilde{r}, \tilde{\theta}, \phi)$ is given by Eq. (III-34):

$$p_{\text{cutoff}}(\bar{\gamma}_c, 1) = \frac{qM}{4\pi \tilde{r}^2} \tilde{\rho}^2(\bar{\gamma}_c, 1) \quad (\text{IV-24})$$

To compute $\tilde{\rho}(\bar{\gamma}_c, 1)$, we recall that $\bar{\gamma}_c$ is a function of particle momentum through λ and ρ_c of Eqs. (IV-12) and (IV-13). Q_c of Eq. (IV-19) is set equal to one and Eqs. (IV-12), (IV-13), and (IV-19) are solved simultaneously by iteration to obtain $\tilde{\rho}(\bar{\gamma}_c, 1)$, given point $(\tilde{r}, \tilde{\theta}, \phi)$ and loop radius, a .

As an example, Figs. 16 and 17 show the flux ratio in the field of a current loop with a radius of ten meters. The points are on the surface of a toroid $\tilde{\rho} = 10$ meters at selected $\tilde{\theta}$. The loop has the same dipole moment as the infinitesimal dipole. We notice that, for the current loop, there is a smaller variation of the cutoff energy with latitude compared to the infinitesimal dipole.

The totally shielded region is oval-shaped for small λ becoming more nearly circular as λ increases. The partially shielded region is also oval-shaped, becoming more circular as λ increases. As λ increases even further, the partially shielded region becomes oval-shaped again, confined to polar angles near the plane of the loop as shown in Fig. 18. Thus, low-energy particles are forbidden to enter a large, flattened doughnut-shaped region around the loop and high-energy particles are forbidden to enter a smaller circular doughnut-shaped region. Figure 18 shows the totally and partially shielded regions in the (ρ', θ) plane for selected λ . The (ρ', θ) coordinate system is a coordinate system in real space in which the forbidden and allowed regions are normalized by the loop radius according to the transformation:

$$\rho' = \frac{\rho}{\lambda} = \frac{r}{a} \quad . \quad (\text{IV-25})$$

Equation (IV-6) becomes

$$Q = \frac{4k^2 C(k)}{\pi\lambda^2 [\rho'^2 + 2\rho' \sin \theta + 1]^{1/2}} + \frac{2\bar{\gamma}}{\lambda\rho' \sin \theta} \quad (\text{IV-26})$$

$$k^2 = \frac{4\rho' \sin \theta}{\rho'^2 + 2\rho' \sin \theta + 1} \quad . \quad (\text{IV-27})$$

The advantage of this coordinate system is that the loop is located at $\rho' = 1$, $\theta = \pi/2$, independent of the loop radius.

The distance, $\Delta\rho'_T$, between the intercepts of the totally shielded region in the plane of the loop is plotted in Fig. 19, reproduced from [11]. As Levy pointed out, the totally shielded region

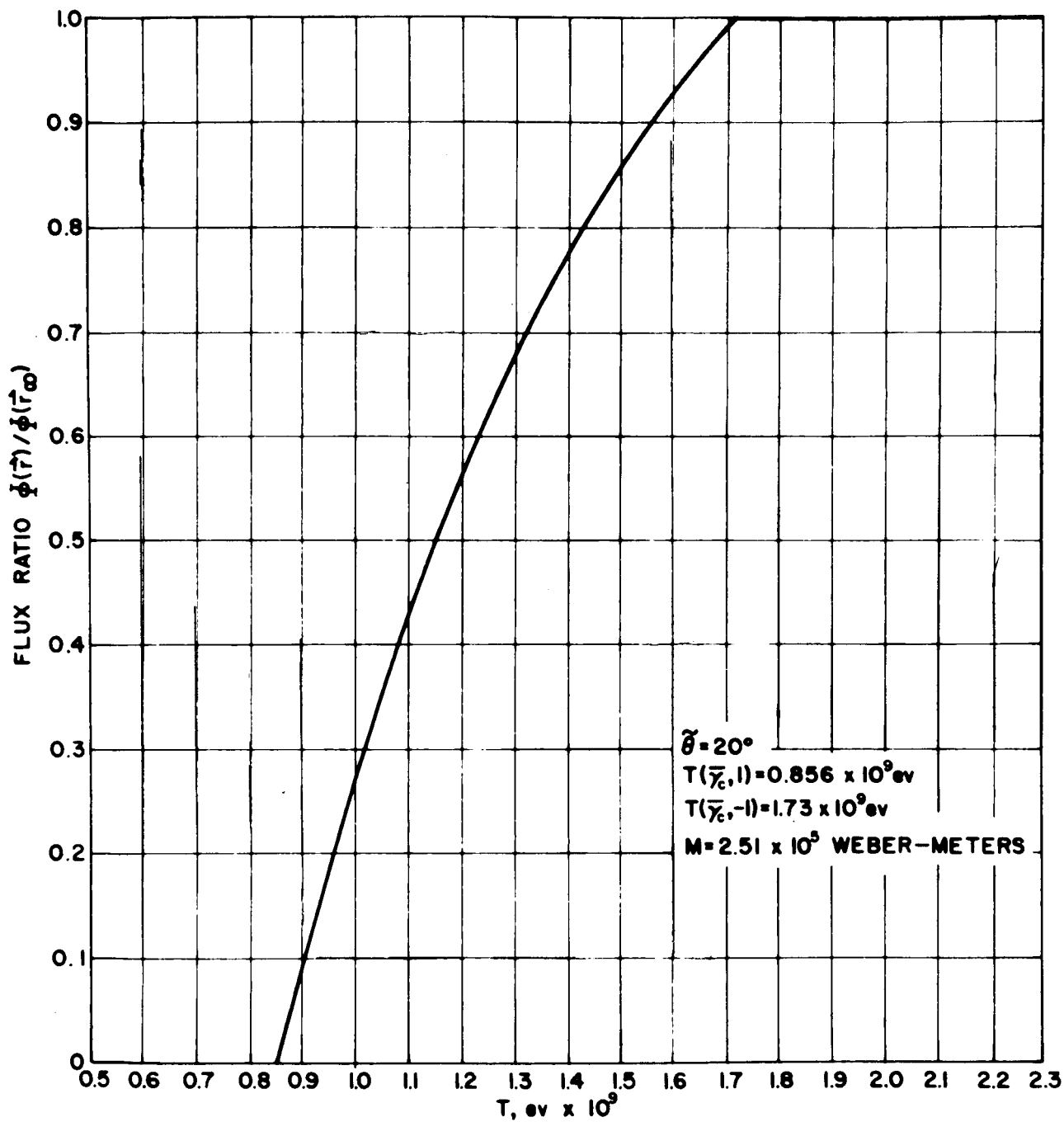


Fig. 16-RELATIVISTIC PROTON FLUX RATIO TEN METERS FROM A CURRENT LOOP WITH A RADIUS OF TEN METERS AT $\tilde{\theta} = 20^\circ$.

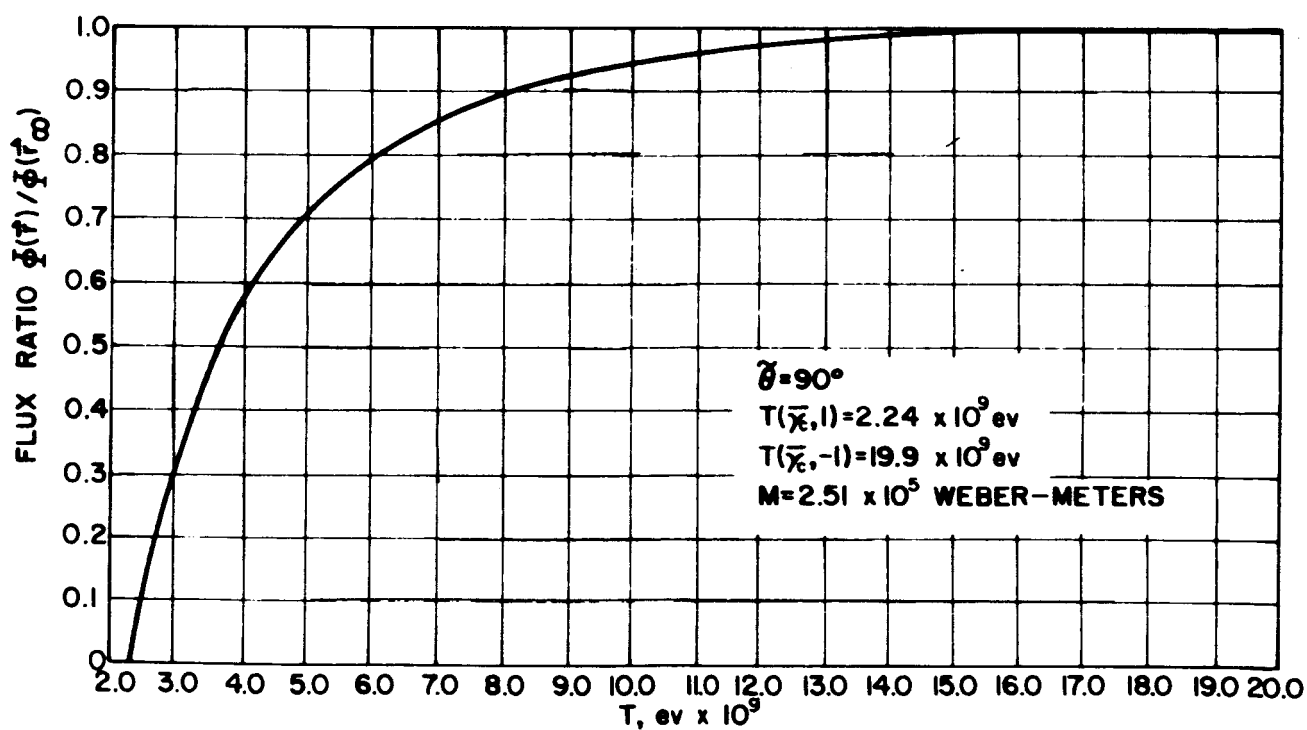
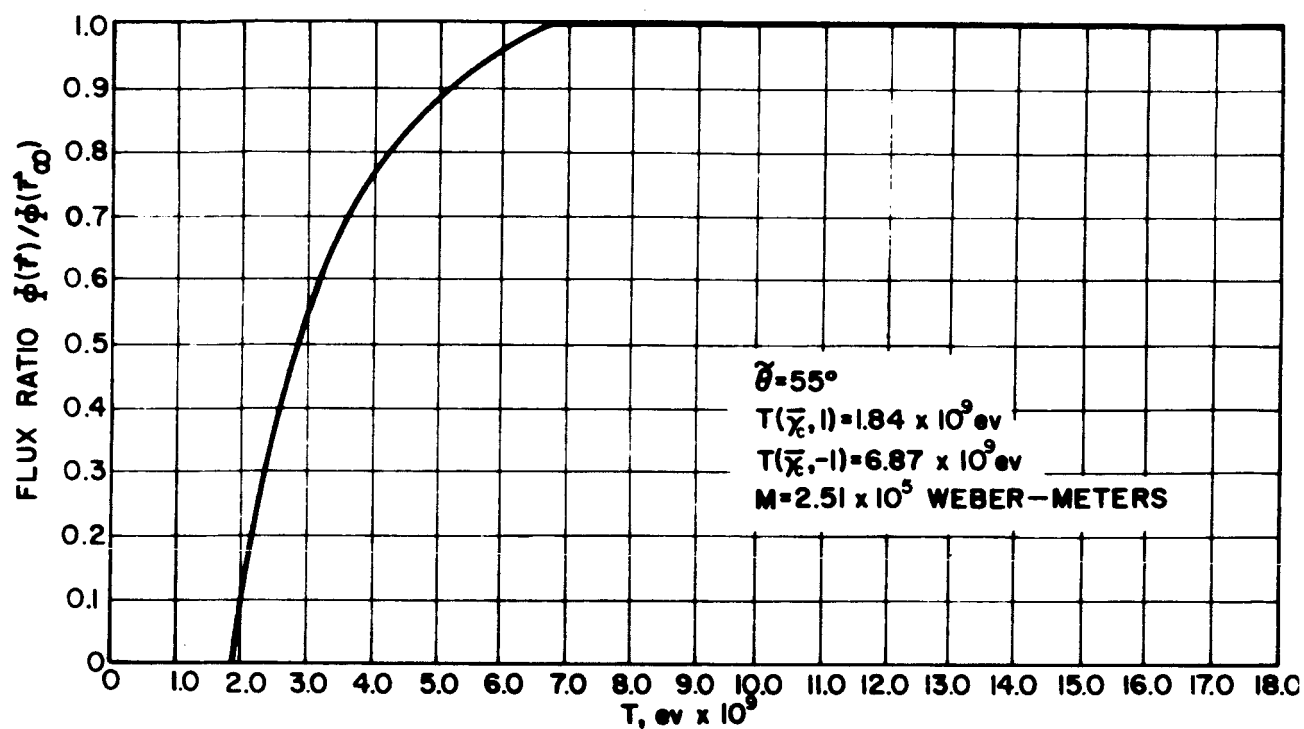


Fig. 17 - RELATIVISTIC PROTON FLUX RATIO TEN METERS FROM A CURRENT LOOP WITH A RADIUS OF TEN METERS AT SELECT θ .

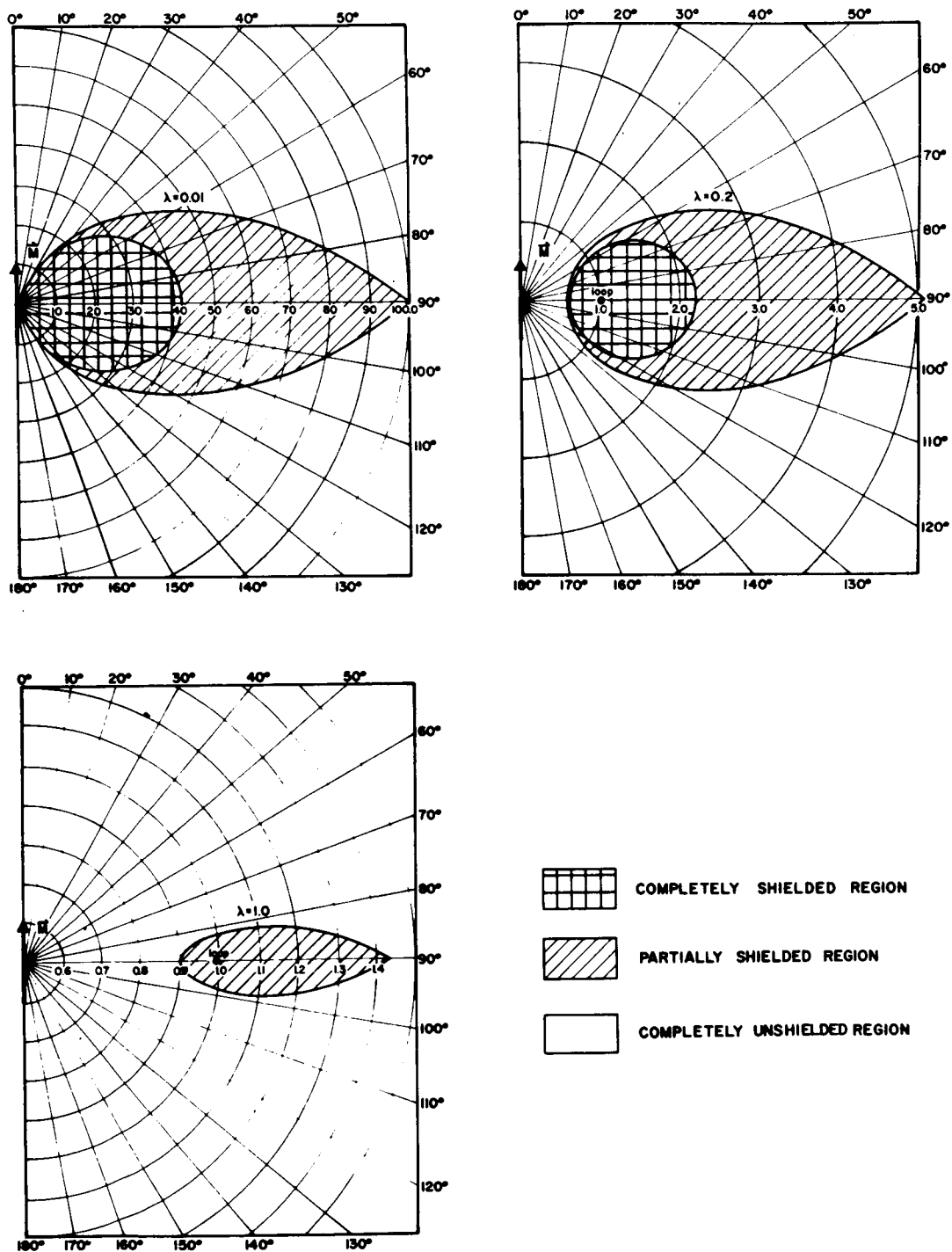


Fig. 18 - SHIELDED REGIONS IN THE (ρ', θ) PLANE
OF A FINITE CURRENT LOOP

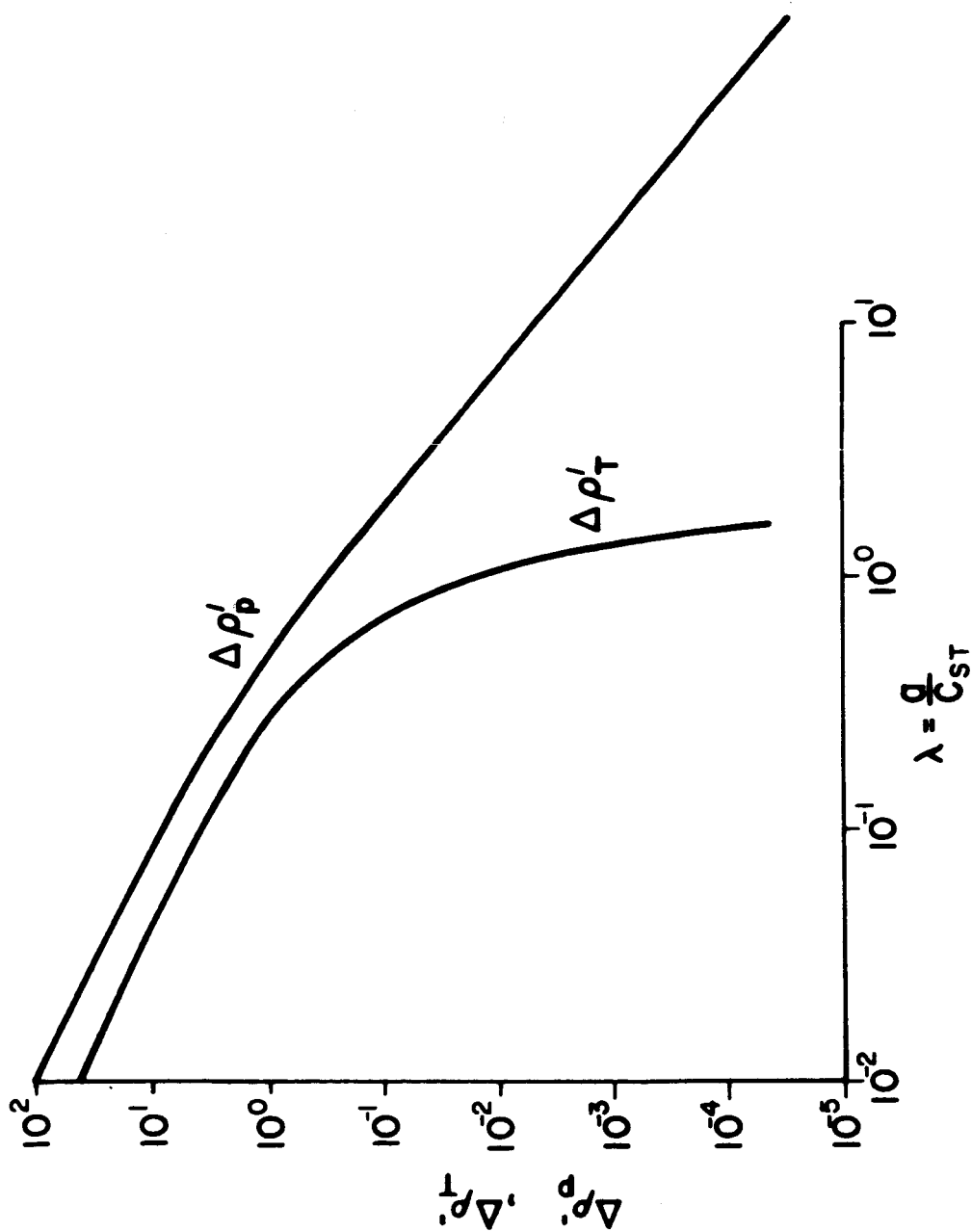
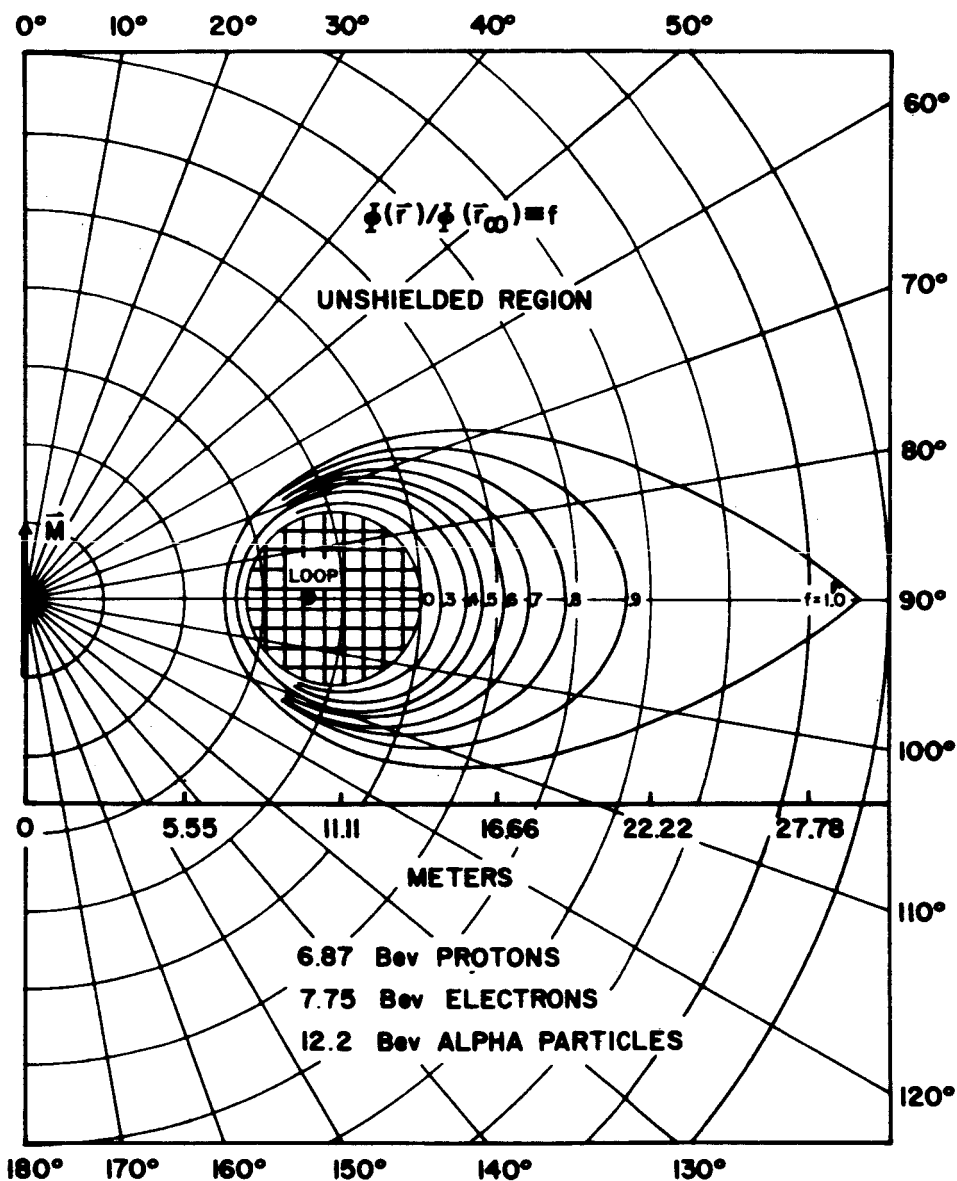


Fig.19 - LIMITS OF THE TOTALLY SHIELDED REGION AND PARTIALLY SHIELDED REGION IN THE PLANE OF THE LOOP.

is largest for small λ , i.e., the loop is more effective as a shield for particles with a large Störmer radius in comparison to the loop radius. The loop is quite effective as an "all or nothing shield" up to $\lambda \approx 1.0$ and then its effectiveness decreases very rapidly with λ . The distance, $\Delta\rho'_P$, between the intercepts of the partially shielded region in the plane of the loop is also plotted in Fig. 19. $\Delta\rho'_P$ decreases slowly with λ and at $\lambda = 1.0$, $\Delta\rho'_P/\Delta\rho'_T \approx 10^2$. For larger λ , this ratio increases very rapidly with increasing λ . We observe that the partially shielded region exists when the totally shielded region has disappeared, and thus assumes an additional importance in the high energy regime where the totally shielded region is so small that it is insignificant.

Figure 20 shows the constant flux contours in the (r, θ) plane of our 10-meter current loop, analogous to Fig. 14, for 6.87 Bev protons and other particles of equal rigidity.



$a = 10$ METERS

$\lambda = 0.36$

$\bar{\gamma}_c = -1.023656$

$M = 2.51 \times 10^6$ WEBER-METERS



TOTALLY SHIELDED
REGION

Fig. 20-CONSTANT FLUX CONTOURS IN THE (r, θ) PLANE FOR UNBOUND CHARGED PARTICLES AROUND A 10 METER CURRENT LOOP WITH A DIPOLE MOMENT $M = 2.51 \times 10^6$ WEBER-METERS.

APPENDIX I

EQUATIONS OF MOTION IN SPHERICAL COORDINATES

The relativistic Hamiltonian for charged particle motion in a static magnetic field is (Ref. 1) :

$$H = [(\vec{P} - q\vec{A})^2 c^2 + m_0^2 c^4]^{\frac{1}{2}} \quad (\text{IA-1})$$

where

$$\vec{P} = P_r \hat{r} + \frac{P_\theta}{r} \hat{\theta} + \frac{P_\phi}{r \sin \theta} \hat{\phi} \quad (\text{IA-2})$$

For our dipole field:

$$\vec{A} = A_\phi(r, \theta) \hat{\phi} . \quad (\text{IA-3})$$

Hamilton's canonical equations provide us with the equations of motion:

$$\dot{r} = \frac{P_r c^2}{H} \quad (\text{IA-4})$$

$$\dot{\theta} = \frac{P_\theta c^2}{r^2 H} \quad (\text{IA-5})$$

$$\dot{\phi} = \frac{c^2}{r H \sin \theta} \left[\frac{P_\phi}{r \sin \theta} - q A_\phi \right] \quad (\text{IA-6})$$

$$\dot{P}_r = \frac{c^2}{H} \left[\frac{P_\theta^2}{r^3} + \left(\frac{P_\phi}{r \sin \theta} - q A_\phi \right) \left(\frac{P_\phi}{r^2 \sin \theta} + q \frac{\partial A_\phi}{\partial r} \right) \right] \quad (\text{IA-7})$$

$$\dot{P}_\theta = \frac{c^2}{H} \left[\frac{P_\phi}{r \sin \theta} - q A_\phi \right] \left[\frac{P_\phi \cos \theta}{r \sin^2 \theta} + q \frac{\partial A_\phi}{\partial \theta} \right] \quad (\text{IA-8})$$

$$\dot{P}_\phi = 0 \quad (\text{IA-9})$$

Since (Ref. 1):

$$\frac{P_i}{h_i} = \frac{p_i}{h_i} + qA_i \quad (\text{IA-10})$$

where P_i is the particle canonical momentum (linear or angular) conjugate to the i^{th} coordinate and p_i is the particle mechanical momentum (linear or angular) conjugate to the i^{th} coordinate; then P_r is the r -component of the linear mechanical momentum and P_θ is the θ -component of the angular mechanical momentum vector. Even though the potential field is velocity dependent, the Hamiltonian is still the total energy and a constant of the motion [1]:

$$H = mc^2 = [p^2 c^2 + m_0^2 c^4]^{\frac{1}{2}}. \quad (\text{IA-11})$$

Since the total energy is a constant of the motion, p is also a constant of the motion. If

$$2\bar{\Gamma} \equiv \frac{-P_\theta}{p} \quad (\text{IA-12})$$

$$\tau \equiv \frac{-P_r}{p} \quad (\text{IA-13})$$

and dividing and multiplying Eqs. (IA-7) and (IA-8) by p^2 , and recalling Eqs. (II-8) and (II-9), Eqs. (IA-7) and (IA-8) become:

$$\dot{P}_r = pv \left[\frac{4\Gamma^2}{r^3} + Q \left(\frac{2\gamma}{r^2 \sin \theta} - \frac{q}{p} \frac{\partial A_\phi}{\partial r} \right) \right] \quad (\text{IA-14})$$

$$\dot{P}_\theta = pvQ \left[\frac{2\gamma \cos \theta}{r \sin^2 \theta} - \frac{q}{p} \frac{\partial A_\phi}{\partial \theta} \right] \quad (\text{IA-15})$$

Solving Eq. (IA-15) simultaneously with Eqs. (IA-4), (IA-5), (IA-6), we obtain:

$$\frac{P_\theta}{p} = - \int \frac{Q}{\tau} \left[\frac{2\gamma \cos \theta}{r \sin^2 \theta} - \frac{q}{p} \frac{\partial A_\phi}{\partial \theta} \right] dr + C_1 \quad (\text{IA-16})$$

$$\left(\frac{P_\theta}{p} \right)^2 = 2 \int Q \left[\frac{2\gamma \cos \theta}{r \sin^2 \theta} - \frac{q}{p} \frac{\partial A_\phi}{\partial \theta} \right] r^2 d\theta + C_2 \quad (\text{IA-17})$$

$$\frac{P_\theta}{p} = - r \phi \sin \theta \left[\frac{2\gamma \cos \theta}{r \sin^2 \theta} - \frac{q}{p} \frac{\partial A_\phi}{\partial \theta} \right] + C_3 \quad (\text{IA-18})$$

If

$$\bar{\Gamma} \equiv \frac{\Gamma}{C_{st}} \quad (\text{IA-19})$$

$$X \equiv \left[\frac{2\bar{\gamma} \cos \theta}{\rho \sin^2 \theta} - \frac{q}{p} \frac{\partial A_\phi}{\partial \theta} \right] \quad (\text{IA-20})$$

the most complete implicit solution for $\bar{\Gamma}$ in Störmer space is:

$$\bar{\Gamma}^2 - \bar{\Gamma} = - \frac{1}{4} \int \frac{Q}{\tau} X d\rho + \frac{1}{2} \int Q X \rho^2 d\theta - \frac{X \rho \phi \sin \theta}{4} + C_0 \quad (\text{IA-21})$$

For our infinitesimal dipole, Eq. (IA-17) may be integrated explicitly and solved simultaneously with Eq. (IA-18):

$$4\bar{\Gamma}^2 - \bar{\Gamma} = - \left[\frac{4\bar{\gamma}^2}{\sin^2 \theta} + \frac{\sin^2 \theta}{\rho^2} \right] + \phi \cos \theta \left[\frac{\sin \theta}{\rho} - \frac{2\bar{\gamma}}{\sin \theta} \right] + C'_3 \quad (\text{IA-22})$$

Equation (IA-22) gives $\bar{\Gamma}$ as a function of particle motion projected onto (θ, ϕ) coordinate surfaces (i.e., surfaces $\rho = \text{constant}$). $-2\bar{\Gamma}$ is the ratio of the θ component of the particle mechanical momentum about the origin of the dipole centered coordinate system to the total

linear momentum, analogous to the impact parameter -2γ at infinity. τ is analogous to Q , and C_i are arbitrary constants.

Solving Eq. (IA-14) simultaneously with Eqs. (IA-4), (IA-5), and (IA-6), we obtain:

$$\left(\frac{P_r}{p}\right)^2 = 8 \int \frac{\bar{\Gamma}^2 d\rho}{\rho^3} + 2 \int Q \left[\frac{2\bar{\gamma}}{\rho^2 \sin \theta} - \frac{q}{p} \frac{\partial A_\phi}{\partial \rho} \right] d\rho + C_4 \quad (\text{IA-23})$$

$$\frac{P_r}{p} = -2 \int \frac{\bar{\Gamma}}{\rho} d\theta - \int \frac{Q}{2\bar{\Gamma}} \left[\frac{2\bar{\gamma}}{\rho^2 \sin \theta} - \frac{q}{p} \frac{\partial A_\phi}{\partial \rho} \right] \rho^2 d\theta + C_5 \quad (\text{IA-24})$$

$$\frac{P_r}{p} = -4 \int \frac{\bar{\Gamma}^2 \sin \theta d\phi}{Q\rho^2} - \phi \left[\frac{2\bar{\gamma}}{\rho} - \frac{q\rho \sin \theta}{p} \frac{\partial A_\phi}{\partial \rho} \right] + C_6 \quad (\text{IA-25})$$

A complete implicit solution analogous to Eq. (IA-22) giving $\tau = \tau(\rho, \theta, \phi, \bar{\gamma}, \bar{\Gamma}, C'_0)$ can be easily derived:

$$Y \equiv \frac{2\bar{\gamma}}{\rho^2 \sin \theta} - \frac{q}{p} \frac{\partial A_\phi}{\partial \rho} \quad (\text{IA-26})$$

$$\begin{aligned} \tau^2 - 2\tau &= 2 \int \left[\frac{4\bar{\Gamma}^2}{\rho^3} + QY \right] d\rho - \int \left[\frac{2\bar{\Gamma}}{\rho} + \frac{QY}{2\bar{\Gamma}} \right] \rho^2 d\theta \\ &\quad - 4 \int \frac{\bar{\Gamma}^2 \sin \theta d\phi}{Q\rho^2} - \phi Y \rho \sin \theta + C'_0 \end{aligned} \quad (\text{IA-27})$$

For the infinitesimal dipole, portions of Eqs. (IA-23), (IA-24), and (IA-25) may be integrated explicitly:

$$\tau^2 = 8 \int \frac{\bar{\Gamma}^2}{\rho^3} d\rho - \frac{4\bar{\gamma}^2}{\rho^2 \sin^2 \theta} - \frac{4\bar{\gamma}}{\rho^3} - \frac{\sin^2 \theta}{\rho^4} + C_4 \quad (\text{IA-28})$$

$$\tau = 2 \int \frac{\bar{\Gamma}}{\rho} d\theta + \int \frac{Q}{\bar{\Gamma}} \left[\frac{\bar{\gamma}}{\sin \theta} + \frac{\sin \theta}{\rho} \right] d\theta - C_5 \quad (\text{IA-29})$$

$$\tau = 4 \int \frac{\bar{\Gamma}^2 \sin \theta}{Q \rho^2} d\phi + \frac{2\phi}{\rho} \left[\bar{\gamma} + \frac{\sin^2 \theta}{\rho} \right] - C_6 \quad (\text{IA-30})$$

τ is the cosine of the angle between the radius vector and the projection of the particle momentum vector onto the meridian plane. Referring to Fig. 1, $\tau = \sin \alpha \cos \beta$. τ , Q , $\bar{\Gamma}$ are related by expressing $\vec{p} \cdot \vec{p}$ in spherical coordinates:

$$1 = \tau^2 + \frac{4 \bar{\Gamma}^2}{\rho^2} + Q^2 \quad (\text{IA-31})$$

Equation (IA-22) may be solved simultaneously with Eqs. (IA-29) and (IA-30) yielding τ explicitly as a function of particle motion projected onto surfaces $\rho = \text{constant}$. Equations (IA-21) and (IA-27) are coupled nonlinear integral equations. Their solution would give τ and $\bar{\Gamma}$ as functions of particle motion in three-dimensional space — a highly desirable solution.

REFERENCES

1. Goldstein, H., Classical Mechanics, Addison-Wesley Publishing Co., Inc., 1959.
2. Störmer, C., The Polar Aurora, Clarendon Press, Oxford, 1955.
3. Swann, W.F.G., "Application of Liouville's Theorem to Electron Orbits in the Earth's Magnetic Field," Phys. Rev. 44, 224-227, 1933.
4. Vallarta, M.S., "Theory of the Geomagnetic Effects of Cosmic Radiation," Handbuch der Physik, Vol. XLVI, Springer-Verlag, Berlin, 1961.
5. Lemaitre, G. and Vallarta, M.S., "On Compton's Latitude Effect of Cosmic Radiation," Phys. Rev. 43, 87-91, 1933.
6. Lemaitre, G. and Vallarta, M.S., "On the Geomagnetic Analysis of Cosmic Radiation," Phys. Rev. 49, 719-726, 1936.
7. Schremp, E.J., "General Theory of the Earth's Shadow Effect of Cosmic Radiation," Phys. Rev. 54, 153-162, 1938.
8. Stratton, J.A., Electromagnetic Theory, McGraw-Hill, New York, New York, 1941.
9. Jahnke, E. and Emde, F., Tables of Functions with Formulae and Curves, Dover Publications, New York, New York, 1945.
10. Urban, E.W., "Charged Particle Motion in Axially Symmetric Magnetic Fields," M.S. Thesis, University of Alabama, 1963.
11. Levy, R.H., "Radiation Shielding of Space Vehicles by Means of Superconducting Coils," Avco-Everett Research Laboratory Research Report 106, 1961.

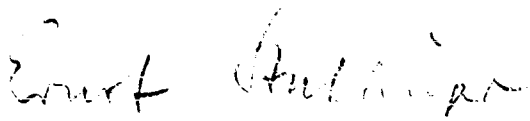
12. Alfvén, H. and Fälthammar, C., Cosmical Electrodynamics, Clarendon Press, Oxford, 1963.
13. Chapman, S. and Ferraro, V., "Terr. Mag. and Atoms," Elec., 45, 1-10, 1941.
14. Treiman, S.B., "Effects of Equatorial Ring Current on Cosmic-Ray Intensity," Phys. Rev. 89, 130-133, 1953.
15. Ray, E.C., "Effects of a Ring Current on Cosmic Radiation," Phys. Rev. 101, 1142-1148, 1956.
16. Sauer, H.H. and Ray, E.C., "On Cosmic Ray Cutoffs," Office of Naval Research Contract N9-ONR-938-1148, 1956.
17. Kellogg, P.J. and Winckler, J.R., "Cosmic Ray Evidence for a Ring Current," J. Geophys. Res. 66, 3991-4001, 1961.
18. Quenby, J.J. and Webber, W.R., "Cosmic Ray Cutoff Rigidities and the Earth's Magnetic Field," Phil. Mag. 4, 90-113, 1958.
19. Lüst, R., "Impact Zones for Solar Cosmic Ray Particles," Phys. Rev. 105, 1827-1839, 1957.
20. Jory, F.S., "Selected Cosmic Ray Orbits in the Earth's Magnetic Field," Phys. Rev. 103, 1068-1075, 1956.
21. Kelsall, T., "Solar Proton Impact Zones," J. Geophys. Res. 66, 4047-4070, 1961.
22. Dow, N.F., "Structural Implications of the Ionizing Radiation in Space," TIS Report R60 SD376, Space Sciences Laboratory, General Electric Co., 1959.
23. Tooper, R.F. and Kash, S.W., "Electromagnetic Shielding Feasibility Study," Armour Research Foundation Report ASD-TDR-63-194, 1963.
24. Brown, G.V., "Magnetic Radiation Shielding," Proceedings of the International Conference on High Magnetic Fields, M.I.T. Press and Wiley and Sons, Inc., 1962.

APPROVAL

DISTRIBUTION OF UNBOUND CHARGED PARTICLES
IN THE STATIC MAGNETIC FIELD OF A DIPOLE

By Arthur D. Prescott

The information in this report has been reviewed for security classification. Review of any information concerning Department of Defense or Atomic Energy Commission programs has been made by the MSFC Security Classification Office. This report, in its entirety, has been determined to be unclassified.



ERNST STUHLINGER
Director, Research Projects Laboratory

DISTRIBUTION

DIR

Dr. von Braun

R-RP

Dr. Stuhlinger

Mr. Heller

Dr. Shelton

Dr. Johnson

Mr. Robinson

Mr. Downey

Mr. Miles

Mr. Urban

Dr. Ashley

Dr. Mechtly

Dr. Dozier

Mr. Holland

Dr. Hale

Mr. Seitz

Mr. Wood

Mr. King

Mr. Potter

Mr. Burrell

Dr. Edmonson

Mr. Stern

Mr. Prescott (25)

Reserve (15)

R-FP

Dr. Ruppe

R-AERO

Dr. Geissler

R-COMP

Dr. Hoelzer

R-QUAL

Mr. Schulze

R-ME

Mr. Kuers

R-TEST

Mr. Heimburg

R-ASTR

Dr. Haeusserman

LVO-DIR

Dr. Debus

R-P&VE

Mr. Jordan

Mr. Whiton

MS-IP

MS-IPL (8)

CC-P

HME-P

MS-H

Scientific and Technical Information
Facility (2)

ATTN: NASA Representative (S-AK/RKT)

P. O. Box 5700

Bethesda, Maryland